Nonlinear Dyn (2023) 111:4375–4393
https://doi.org/10.1007/s11071-022-08096-w

ORIGINAL PAPER

Practical finite-time adaptive neural networks control for incommensurate fractional-order nonlinear systems

Boqiang Cao · Xiaobing Nie · Jinde Cao · Peiyong Duan

Received: 3 May 2022 / Accepted: 8 November 2022 / Published online: 24 November 2022

Abstract The issue associated with the practical finite-time adaptive neural networks control is studied in this paper for a class of incommensurate fractional-order nonlinear systems with external disturbances. With the help of a practical finite-time stability criterion for an integer-order system, the criterion for a fractional-order system is first established, where only the first-order derivative is adopted instead of the fractional-order derivative of the Lyapunov function. This provides an avenue to address the practical finite-time adaptive control problem for incommensurate fractional-order systems. By using the property of fractional-order calculus, a practical finite-time adaptive control scheme is then designed, which is the first time that a practical finite-time adaptive control problem for an incommensurate fractional-order nonlinear system has been considered. In contrast with the control schemes in the literature, the control signals in this paper are generated by some filters, with the result that the fluctuation range of control signals is reduced (especially around the initial time). In addition, a compensated signal is introduced into the design processes of the control scheme, which can not only compensate for the difference caused by the filter of the control scheme, but also simplify the design processes of the control scheme and stability analysis of the controlled system. Finally, numerical simulations and some comparisons are presented to illustrate the effectiveness of the proposed practical finite-time control scheme.

Keywords Finite-time adaptive control · Incommensurate fractional-order system · Lyapunov functional approach · External disturbance

B. Cao · X. Nie (✉)
School of Mathematics, Southeast University, Nanjing 211189, China
e-mail: xbnie@seu.edu.cn

B.Cao
e-mail: boqiangcao@sina.com

J. Cao
School of Mathematics, Frontiers Science Center for Mobile Information Communication and Security, Southeast University, Nanjing 210096, China
e-mail: jdcao@seu.edu.cn

J. Cao
Purple Mountain Laboratories, Nanjing 211111, China

J. Cao
Yonsei Frontier Lab, Yonsei University, Seoul 03722, South Korea

P. Duan
School of Mathematics and Information Sciences, Yantai University, Yantai 264005, China
e-mail: duanpeiyong@ytu.edu.cn

1 Introduction

Fractional-order calculus, as a global concept, is very suitable to describe the memory and heredity properties of various processes and materials, which is completely neglected by the traditional integer-order derivative. In recent years, with the development of fractional-order calculus theory, an increasing number of practical phe-

nomena have been modeled by fractional-order systems to improve modeling accuracy in many research fields, such as biology, engineering, electroanalytical chemistry and physics [1–3]. The stability of a system is one of the most important dynamic characteristics, which has attracted the attention of many scholars, and there are many excellent research results with regards to stability, synchronization and so on [4,5]. Many practical systems are usually unstable or chaotic, and thus, it is necessary to introduce some intervention measures to aid systems in achieving the actual requirement. Thus, numerous control schemes have been proposed in recent years, such as synchronization control [4] and adaptive control [6–10].

Adaptive control, which is a classical and important control method, has been successfully applied in integer-order systems based on the backstepping method in the past few years [6,7,10–15]. For example, the adaptive control schemes were designed in [11,12] for strict feedback systems, where the control direction was assumed to be unknown in [11,12]. Furthermore, adaptive control schemes for nonstrict feedback nonlinear systems were designed in [13,16] by using the property of radial basis function neural networks. Since then, many results about nonstrict feedback nonlinear systems that consider Markov jumps, input delays, actuator failures or input dead-zones [7,14,15,17] have emerged. Recently, with the rapid development of research on fractional-order calculus, the adaptive control method has also been extended to fractional-order systems (FOSs) [8,18–22]. For example, the observer-based adaptive control scheme was designed in [8] by constructing a fractional-order state observer. Liu et al. [20] designed a composite learning adaptive control scheme with the help of the dynamic surface technique. The authors in [22] proposed the notion of the Mittag–Leffler input-to-state practical stable Lyapunov function and designed an event-triggered adaptive control scheme for FOSs with unmodeled dynamics. The systems in the aforementioned literature are commensurate FOSs, which is a special case of incommensurate FOSs, i.e., the derivative orders of each equation in the system are not completely equal. Therefore, the adaptive control scheme for a commensurate FOS cannot be directly extended to that of an incommensurate FOS, which is mainly because the equations with unequal derivative order cannot be substituted into the fractional-order derivative of the Lyapunov function. For this reason, the authors in [23] introduced a disturbance-like assumption to solve the finite-time consensus tracking problem for incommensurate FOSs; the issue of practical fixed-time bipartite consensus was studied for incommensurate FOSs in [24] by introducing a sliding-mode manifold; some authors [9,25,26] also transformed the adaptive control problem for incommensurate FOSs into that of integer-order systems by using a frequency distributed model. However, as pointed out in [27], whether the same weighting function $\mu_\alpha(\omega) = \frac{\sin \alpha\pi}{\pi \omega^\alpha}$ can be adopted for different systems is still not strictly proved. In addition, the sign function was involved in the virtual and final controllers in [25,26], which leads to not only the controllers being discontinuous but also the chatting phenomenon appearing in the applications. Furthermore, during the i-th step of the backstepping method, the $(i-1)$-th tracking error appeared in the i-th virtual controller, which makes the structure of the controller complex and difficult for practical use. Therefore, we hope some progress in the controller design will be made for incommensurate FOSs to overcome the above-mentioned shortcomings and avoid the use of the frequency distributed model, which is one of the motivations of this paper.

On the other hand, the convergence rate is also an important performance indicator for practical systems. The control schemes in most of the aforementioned literature were proposed based on the asymptotic stability theory [6,7,11–15]. That is, the preset control objective can be achieved, or the tracking error enters a given region with a long convergence time. In fact, regarding the actual requirement, the control goal is expected to be achieved in finite time, which promotes the development of finite-time stability theory [28,29]. As a more general notion, practical finite-time stability was proposed by Zhu et al. in [30], and some significant results about practical finite-time stability have emerged [31–33]. For example, a criterion for practical finite-time stability was developed in [31]; then, the authors designed a finite-time adaptive control scheme for a class of nonlinear systems by using a command filter technique. In [33], an adaptive control scheme for a multi-agent system was designed based on the proposed fast finite-time stability criterion. In recent years, some finite-time control schemes have also been proposed for FOSs [3,34–36]. The finite-time adaptive sliding mode control schemes were designed in [3,34] for fractional-order nonlinear systems and fractional-order hydro-turbine gov-

erning systems. The finite-time synchronization was studied for fractional memristive neural networks in [35]. Among the many studies of finite-time control for FOSs, the formula $\mathcal{D}^{\alpha} g^{\iota}(t) = \frac{\Gamma(1+\iota)}{\Gamma(1+\iota+\alpha)} g^{\iota-\alpha}(t)\mathcal{D}^{\alpha} g(t)$ ($\iota \in \mathbb{R}, \alpha \in (0,1)$) plays a crucial role in obtaining the results of finite-time control. Unfortunately, as pointed out in [4], this crucial formula may be incorrect (a counterexample is given in [4]). To the best of our current knowledge, when $\iota \in (0,1)$ and $\alpha \in (0,1)$, it is very difficult and even impossible to obtain the relationship $\mathcal{D}^{\alpha} g^{\iota}(t) \leq c_1 g^{c_2}(t)\mathcal{D}^{\alpha} g(t)$, because the fractional-order derivative of the compound function is an infinite series of some complicated functions (see [1, Section 2.7.3]), where $c_1 > 0$ and c_2 are two constants. Therefore, bypassing this incorrect formula and solving the finite-time adaptive tracking control problem of FOSs are a challenging problem. In addition, even if an alternative criterion is obtained, designing a practical finite-time control scheme and proving the stability of the controlled system are also difficult. All these challenging problems are another motivation of this paper.

Motivated by the above discussions, in this paper, we design a practical finite-time adaptive neural networks control scheme for a class of incommensurate FOSs based on the backstepping method, where the external disturbance is considered. The main contributions of this paper can be summarized as follows:

(i) Motivated by the criterion of finite-time control for an integer-order system in [31], the criterion of practical finite-time control for the FOS is established, where only the first-order derivative is adopted instead of the fractional-order derivative of the Lyapunov function. The merits of this criterion lie in two aspects: it provides a way to deal with the control problem for incommensurate FOSs, and the frequency distribution model adopted in [9,25,26] is avoided, which indicates that the shortcoming of the frequency distribution model is also overcome. In addition, it is worth pointing out that practical finite-time stability can be achieved for the FOS in this paper by using only the same conditions for the Lyapunov function as those for the integer-order system in [31].

(ii) A novel practical finite-time adaptive neural networks control scheme is proposed in this paper for incommensurate FOSs. The proposed practical finite-time control scheme can also be degenerated into a non-finite time control scheme for commensurate/incommensurate FOSs, which, compared with the literature [9,18,20–22,36,37], is also novel and can be used to control both incommensurate and commensurate FOSs in [9,18,20–22,36,37].

(iii) In contrast with the results in [18,36,37], in this paper, the virtual and final control signals are generated by some designed filters during the design processes of the control scheme, which can reduce the fluctuation range of control signals, especially around the initial time (see Remarks 9 and 11). Additionally, to compensate for the difference between the original signal (i.e., $h_i(t)$) and the control signal, a compensated signal is introduced, which simplifies the processes of control scheme design and stability analysis.

The rest of this paper is organized as follows: In Sect. 2, some preliminary results are presented, and the problems to be studied are also formulated; The practical finite-time adaptive neural networks control scheme is designed in Sect. 3; Two numerical examples are provided in Sect. 4 to illustrate the effectiveness of proposed adaptive control scheme; A summary is presented in Sect. 5.

Notations: $\mathbb{N} = \{0, 1, 2, \cdots\}$ is the set of natural numbers, $\mathbb{N}_+ = \mathbb{N} \setminus \{0\}$, and $\mathbb{R}^n$ is the Euclidean space with dimension n. $\mathcal{C}^m([0,+\infty), \mathbb{R})$ consists of functions from $[0,+\infty)$ to $\mathbb{R}$ that have $m \in \mathbb{N}$ order continuous derivatives. $\|\cdot\|$ denotes the Euclidean norm of the vector. For vector $x = (x_1, \ldots, x_n)^{\mathrm{T}} \in \mathbb{R}^n$, $\bar{x}_i \triangleq (x_1, \ldots, x_i)^{\mathrm{T}}$.

2 Preliminaries and problem formulation

2.1 Preliminaries

In this subsection, we first present the fractional-order calculus and some related results.

Definition 1 [1] For function $f(t) \in \mathcal{C}^m([0,+\infty), \mathbb{R})$, its Caputo-type fractional-order derivative with order $\alpha > 0$ is defined as

$$\mathcal{D}^{\alpha} f(t) = \frac{1}{\Gamma(m-\alpha)} \int_0^t \frac{f^{(m)}(\tau)}{(t-\tau)^{\alpha+1-m}} \mathrm{d}\tau,$$

where m is a positive integer satisfying $m-1 < \alpha \leq m$ and $\Gamma(\cdot)$ is the Gamma function.

Lemma 1 [38] *For function $f(t) \in \mathcal{C}^m([0,+\infty),\mathbb{R})$ with $m \in \mathbb{N}_+$ and $\alpha_1, \alpha_2 > 0$, if there exists $\bar{m} \in \mathbb{N}_+$ with $\bar{m} \le m$ such that $\alpha_2, \alpha_1+\alpha_2 \in [\bar{m}-1, \bar{m}]$, then the following property holds*

$$\mathcal{D}^{\alpha_1}\mathcal{D}^{\alpha_2} f(t) = \mathcal{D}^{\alpha_1+\alpha_2} f(t).$$

Definition 2 [1] The Mittag–Leffler function with one parameter $\alpha > 0$ is defined as

$$E_\alpha(\varsigma) = \sum_{s=0}^{\infty} \frac{\varsigma^s}{\Gamma(\alpha s+1)},$$

where ς is a complex number.

Lemma 2 [13] *For any positive number ζ and $\omega \in \mathbb{R}$, the following inequality holds*

$$0 \le |\omega| - \omega \tanh\frac{\omega}{\zeta} \le \zeta\rho,$$

where $\rho \approx 0.2785$ is positive root of the equation $\rho = e^{-(\rho+1)}$.

Lemma 3 [33] *For any $x_1, x_2 \in \mathbb{R}$ and $r = \frac{r_1}{r_2} \in (0,1)$ with positive odd integers r_1, r_2, the inequality $x_1 x_2^r \le -b_1 x_1^{1+r} + b_2(x_1+x_2)^{1+r}$ holds, where $b_1 = \frac{1}{1+r}(2^{r-1} - 2^{r^2-1})$ and $b_2 = \frac{1}{1+r}\big(1 - 2^{r-1} + \frac{r}{1+r} + \frac{1}{1+r}2^{r(1-r^2)}\big)$.*

Lemma 4 [31] *For $x_s \in \mathbb{R}$, $s = 1, \ldots, n$ and $0 < r < 1$, the following inequality holds*

$$\left(\sum_{s=1}^{n} |x_s|\right)^r \le \sum_{s=1}^{n} |x_s|^r \le n^{1-r}\left(\sum_{s=1}^{n} |x_s|\right)^r.$$

Lemma 5 *For FOS $\mathcal{D}^\alpha x(t) = f(x(t))$, if there exists a continuous and positive definite function $V(x(t))$ such that $\dot{V}(x(t)) \le -q_1 V(x(t)) - q_2 V^\iota(x(t)) + q_3$ with constants $q_1, q_2, q_3 > 0$ and $0 < \iota < 1$, then the trajectory of FOS $\mathcal{D}^\alpha x(t) = f(x(t))$ is practical finite-time stable, and there exists a finite-time T satisfying*

$$T = \max\left\{\frac{1}{\varrho q_1(1-\iota)} \ln\frac{\varrho q_1 V^{1-\iota}(x(0)) + q_2}{q_2}, \frac{1}{q_1(1-\iota)} \ln\frac{q_1 V^{1-\iota}(x(0)) + \varrho q_2}{\varrho q_2}\right\} \tag{1}$$

such that for any $t \ge T$, the following inequality holds

$$V(x(t)) \le \min\left\{\frac{q_3}{(1-\varrho)q_1}, \left(\frac{q_3}{(1-\varrho)q_2}\right)^{1/\iota}\right\},$$

where $0 < \varrho < 1$ is an arbitrary constant.

Proof The results can be proven by using an argument similar to that in [31], so we omit it here. □

Remark 1 In this paper, the definition of practical finite-time stability is adopted; namely, for any initial value $x(0) = x_0$, there exist $\varepsilon > 0$ and $T(\varepsilon, x_0) < \infty$, such that the solution of system satisfies $\|x(t)\| \le \varepsilon$ for all $t \ge T$. If we let $\varepsilon = 0$, then the above definition will degenerate to the definition of finite-time stability that was adopted in [3,28,29]. Besides, there is another definition of finite-time stability in [39]: for constants $0 < \varepsilon_1 < \varepsilon_2$ and finite-time $T > 0$, $\|x_0\| \le \varepsilon_1$ implies $\|x(t)\| \le \varepsilon_2$ for $\forall t \in [0, T]$. Thus, we can see that the former definition of finite-time stability mainly focuses on whether the solution of the system converges to zero at T and is always equal to zero on the interval $(T, +\infty)$, whereas the latter definition of finite-time stability focuses on the boundedness of solution on the finite interval $[0, T]$.

2.2 Problem formulation

Consider the following incommensurate fractional-order nonlinear system

$$\begin{cases} \mathcal{D}^{\alpha_i} x_i = x_{i+1} + f_i(x) + \Delta_i(t), \\ \mathcal{D}^{\alpha_n} x_n = u + f_n(x) + \Delta_n(t), \\ y = x_1, \quad i = 1, \ldots, n-1, \end{cases} \tag{2}$$

where $\alpha_s \in (0,1)$ $(s = 1, \ldots, n)$, x_s is the state variable, u and y are the input and output of the system, respectively. $f_s(x)$ is an unknown smooth function with $1 + \partial f_s(x)/\partial x_{s+1} \ne 0$ $(s = 1, \ldots, n-1)$, and $\Delta_s(t)$ is the external disturbance.

Remark 2 System (2) is a classical incommensurate fractional-order one with the nonstrict feedback form, which can characterize many practical systems, such as fractional-order Chua–Hartley's system, fractional-order Rössler's system, fractional-order Chen's system, fractional-order Lorenz's system, fractional-order Lotka-Volterra system [1,2]. Meanwhile, (2) also contains numerous systems in the literature as special cases. For example, if $\alpha_1 = \cdots = \alpha_n \in (0,1)$, system (2) becomes the commensurate fractional-order one with the nonstrict feedback form, which was studied in [8,19,37], and if further letting $f_i(x) = f_i(\bar{x}_i)$, system (2) degenerates into the one with the strict feedback form in [18,21]. If $\alpha_1 = \cdots = \alpha_n = 1$, system

(2) becomes an integer-order one, which was considered in [13,14]. Besides, if we use the transformation method in [17], then the systems in [7,20,22,40] can transformed into the special cases of the system (2). Therefore, the design of control scheme for the system (2) is of great significance from both the practical and theoretical points of view.

The control objective of this paper is to design a practical finite-time control scheme such that: (i) all signals in the closed-loop system are bounded; (ii) the system output can track the reference signal $y_d(t)$ with a small error and the tracking error can enter a small region in finite time.

To realize the control objective, the following assumptions are needed.

Assumption 1 The external disturbance $\Delta_i(t)$ $(i = 1, \ldots, n)$ and its derivative are continuous and bounded.

Assumption 2 The reference signal y_d and its derivative are continuous and bounded.

Assumption 3 The orders of fractional derivative in system (2) satisfy $\alpha_i + \alpha_{i+1} \geq 1$ $(i = 1, \ldots, n-1)$.

Remark 3 In some existing literature [19–21], the external disturbance is assumed to be bounded, which is standard. During the design process of the practical finite-time control scheme, it also requires that $\mathcal{D}^{1-\alpha_i}\Delta_i(t)$ is bounded, while it is difficult to verify. Therefore, we assume that $\dot{\Delta}_i(t)$ is bounded, which is an easily verifiable hypothesis and implies the boundedness of $\mathcal{D}^{1-\alpha_i}\Delta_i(t)$. In fact, since $\mathcal{D}^{\alpha}\Delta_i(t)$ is continuous with respect to α, and $\mathcal{D}^1\Delta_i(t) = \dot{\Delta}_i(t)$ and $\mathcal{D}^0\Delta_i(t) = \Delta_i(t)$ are bounded, we can conclude that $\mathcal{D}^{1-\alpha_i}\Delta_i(t)$ is bounded. Assumption 2 is quite standard, which is adopted in many previous studies [7,14,15]. It should be pointed out that $\mathcal{D}^{\alpha}y_d$ $(\alpha \in (0, 1))$ is assumed to be bounded in [19,20,22], which is difficult to verify due to the complexity of fractional-order calculus, while Assumption 2, as an alternative, is easy to verify and implies the boundedness of $\mathcal{D}^{\alpha}y_d$ based on the continuity of fractional-order derivative with respect to order α. We give Assumption 3 to ensure the continuity of $\mathcal{D}^{1-\alpha_i}x_{i+1}$ that will appear during the designing process of the adaptive control scheme. In Assumption 3, there are some constraints to the orders α_i $(i = 1, \ldots, n)$, while it does not seriously influence the actual application, since we find that many practical systems mentioned in [1,2] and references therein can satisfy Assumption 3.

2.3 Radial basis function neural networks

Since the function $f_s(x)$ is unknown and some terms during the design process of the control scheme are difficult to deal with, the radial basis function neural networks are introduced in this subsection to approximate them.

For continuous function $\mathcal{H}(Z) : \mathbb{R}^{n_1} \to \mathbb{R}$ with $n_1 \in \mathbb{N}_+$, we construct the neural networks as $\mathcal{H}_{NN} = W^{\mathrm{T}}\Phi(Z)$, where $Z \in \Omega \subset \mathbb{R}^{n_1}$ is the input of neural networks, $W \in \mathbb{R}^{n_2}$ is the weight vector, n_2 is the number of nodes in neural networks, and $\Phi(Z) = (\phi_1(Z), \ldots, \phi_{n_2}(Z))$ is the Gaussian-like radial basis function vector with

$$\phi_s(Z) = \exp\left[-\frac{(Z-\varpi_s)^{\mathrm{T}}(Z-\varpi_s)}{\delta_s^2}\right],$$

$s = 1, \ldots, n_2$, $\varpi_s = (\varpi_{s1}, \ldots, \varpi_{sn_1})^{\mathrm{T}}$ and δ_s are the center of receptive domain and the width of Gaussian function, respectively.

Lemma 6 [41] *If the nodes number n_2 of neural networks is sufficiently large, then the radial basis function neural networks $\mathcal{H}_{NN} = W^{\mathrm{T}}\Phi(Z)$ can approximate the continuous function $\mathcal{H}(Z)$ over compact set $\Omega \subset \mathbb{R}^{n_1}$ to arbitrary accuracy $\tilde{\epsilon}$ as*

$$\mathcal{H}(Z) = W^{*T}\Phi(Z) + \epsilon(Z),$$

where $W^* \in \mathbb{R}^{n_2}$ is the ideal weight vector of neural networks defined as

$$W^* = \arg\min_{W\in\mathbb{R}^{n_2}}\left\{\sup_{Z\in\Omega}|\mathcal{H}(Z) - W^{\mathrm{T}}\Phi(Z)|\right\},$$

and $\epsilon(Z)$ is the approximation error satisfying $|\epsilon(Z)| < \tilde{\epsilon}$.

Lemma 7 [15] *Let $Z = (z_1, \ldots, z_{n_1})^{\mathrm{T}}$, ϖ_s and $\Phi(Z)$ are defined as in Lemma 6, $\check{Z} = (z_{i_1}, \ldots, z_{i_\hbar})^{\mathrm{T}}$, $\check{\varpi}_s = (\varpi_{s,i_1}, \ldots, \varpi_{s,i_\hbar})^{\mathrm{T}}$, and $\{i_1, \ldots, i_\hbar\}$ is a subsequence of $\{1, \ldots, n_1\}$. $\check{\Phi}(\check{Z}) = (\check{\phi}_1(\check{Z}), \ldots, \check{\phi}_{n_2}(\check{Z}))$ with $\check{\phi}_s(\check{Z}) = \exp\left[-\frac{(\check{Z}-\check{\varpi}_s)^{\mathrm{T}}(\check{Z}-\check{\varpi}_s)}{\delta_s^2}\right]$, $s = 1, \ldots, n_2$ are radial basis function vectors. Then,*

$$\|\Phi(Z)\| \leq \|\check{\Phi}(\check{Z})\|.$$

For the sake of simplicity, $\check{\Phi}(\check{Z})$ is still denoted by $\Phi(\check{Z})$ in the following if no confusion arises.

3 The design of control scheme and stability analysis

This section is devoted to designing the practical finite-time adaptive neural networks control scheme for system (2) and analyzing the stability of the controlled system. In order to do this, we first define the following coordinate transform

$$\begin{cases} z_1 = x_1 - y_d, \\ z_i = x_i - \chi_{i-1}, \quad i = 2, \ldots, n, \end{cases} \tag{3}$$

where χ_i, $(i = 1, \ldots, n-1)$ is the virtual control signal that will be specified later. The control scheme is designed in the following by using the backstepping technique.

Step 1: According to (2) and (3), and using Lemma 1, we have

$$\begin{aligned} \dot{z}_1 &= \mathcal{D}^{1-\alpha_1}\mathcal{D}^{\alpha_1}x_1 - \dot{y}_d \\ &= \mathcal{D}^{1-\alpha_1}(z_2 + \chi_1 + f_1(x) + \Delta_1(t)) - \dot{y}_d. \end{aligned} \tag{4}$$

Since the fractional-order derivative of χ_1 with order $(1-\alpha_1)$ is appeared in (4), the virtual control signal χ_1 is difficult to design. Thus, motivated by the dynamic surface technique [20], we define the following fractional filter

$$\mathcal{D}^{1-\alpha_1}\chi_1(t) = -\kappa_1(\chi_1(t) - h_1(t)), \chi_1(0) = 0, \tag{5}$$

where $h_1(t)$ is an intermediate signal that will be designed later and $\kappa_1 > 0$ is a designed parameter. From (5), we can only obtain that the error $\tilde{h}_1 = \chi_1 - h_1$ is bounded by a constant (see Lemma 8), but it cannot be guaranteed to converge to a small region of origin. Therefore, we design a compensated signal $\tilde{\chi}_1$ as follows

$$\begin{aligned} &\dot{\tilde{\chi}}_1(t) = -\lambda_1\tilde{\chi}_1(t) - \bar{\lambda}_1\tilde{\chi}_1^r(t) - \kappa_1\chi_1(t), \\ &\tilde{\chi}_1(0) = z_1(0), \end{aligned} \tag{6}$$

where $\lambda_1, \bar{\lambda}_1 > 0$ are the designed parameters and $r = \frac{r_1}{r_2} \in (0, 1)$ with positive odd numbers r_1, r_2. The compensated tracking error is defined as

$$\tilde{z}_1 = z_1 - \tilde{\chi}_1. \tag{7}$$

It then follows from (4) and (7) that

$$\begin{aligned} \dot{\tilde{z}}_1 &= \dot{z}_1 - \dot{\tilde{\chi}}_1 \\ &= \mathcal{D}^{1-\alpha_1}(z_2 + \chi_1 + f_1(x) + \Delta_1(t)) - \dot{y}_d - \dot{\tilde{\chi}}_1. \end{aligned}$$

Based on Assumption 1, there exists a positive constant d_1 such that $|\mathcal{D}^{1-\alpha_1}\Delta_1(t)| \le d_1$, which, together with Lemma 2, implies that

$$\tilde{z}_1\mathcal{D}^{1-\alpha_1}\Delta_1(t) \le d_1|\tilde{z}_1| \le d_1\tilde{z}_1\tanh\left(\frac{d_1\tilde{z}_1}{\zeta_1}\right) + \zeta_1\rho, \tag{8}$$

where $\zeta_1 > 0$ is a designed parameter. Construct the Lyapunov function as

$$V_1 = \frac{1}{2}\tilde{z}_1^2 + \frac{1}{2\eta_1}\tilde{\theta}_1^2,$$

where $\eta_1 > 0$ is a designed parameter, $\tilde{\theta}_1 = \hat{\theta}_1 - \theta_1$ is the estimation error of $\theta_1 = \|W_1^*\|^2$, $\hat{\theta}_1$ is the estimate of θ_1, and W_1^* will be specified later. By using (8), the derivative of V_1 can be calculated as

$$\begin{aligned} \dot{V}_1 =& \tilde{z}_1\big(\mathcal{D}^{1-\alpha_1}(z_2 + \chi_1 + f_1(x) + \Delta_1(t)) \\ &- \dot{y}_d - \dot{\tilde{\chi}}_1\big) + \frac{1}{\eta_1}\tilde{\theta}_1\dot{\hat{\theta}}_1 \\ \le& \tilde{z}_1\mathcal{H}_1(Z_1) + \tilde{z}_1\mathcal{D}^{1-\alpha_1}\chi_1 - \tilde{z}_1\dot{\tilde{\chi}}_1 + \frac{1}{\eta_1}\tilde{\theta}_1\dot{\hat{\theta}}_1 \\ &+ \zeta_1\rho - \lambda_1 z_1\tilde{z}_1 - \bar{\lambda}_1\tilde{z}_1\tilde{\chi}_1^r, \end{aligned}$$

where $\mathcal{H}_1(Z_1) = \mathcal{D}^{1-\alpha_1}(z_2 + f_1(x)) + d_1\tanh\left(\frac{d_1\tilde{z}_1}{\zeta_1}\right) - \dot{y}_d + \lambda_1 z_1 + \bar{\lambda}_1\tilde{\chi}_1^r$ with $Z_1 = (x^{\mathrm{T}}, \hat{\theta}_1, \tilde{\chi}_1, y_d, \dot{y}_d)^{\mathrm{T}} \in \mathbb{R}^{n+4}$. It should be pointed out that $\mathcal{D}^{1-\alpha_1}(z_2 + f_1(x))$ is a continuous function, which thus can be approximated subsequently by using neural networks. In fact, since $\mathcal{D}^{\alpha_2}x_2$ is continuous (from system (2)) and $\alpha_2 \ge 1-\alpha_1$ (according to Assumption 3), we can conclude that $\mathcal{D}^{1-\alpha_1}x_2$ is continuous. Besides, from (5), we obtain that $\mathcal{D}^{1-\alpha_1}\chi_1$ is continuous. Thus, equation $\mathcal{D}^{1-\alpha_1}z_2 = \mathcal{D}^{1-\alpha_1}(x_2 - \chi_1)$ implies that $\mathcal{D}^{1-\alpha_1}z_2$ is continuous. In addition, since $f_1(x)$ is smooth, $\mathcal{D}^{1-\alpha_1}f_1(x)$ is continuous. Based on Lemma 6, the continuous function $\mathcal{H}_1(Z_1)$ can be approximated as

$$\mathcal{H}_1(Z_1) = W_1^{*T}\Phi_1(Z_1) + \epsilon_1(Z_1),$$

where W_1^* is the ideal weight vector and $\epsilon_1(Z_1)$ is the approximation error with $|\epsilon_1(Z_1)| < \tilde{\epsilon}_1$. It then follows from Lemma 7 that

$$\begin{aligned} \tilde{z}_1\mathcal{H}_1(Z_1) &\le |\tilde{z}_1|(\|W_1^*\|\|\Phi_1(Z_1)\| + |\epsilon_1(Z_1))| \\ &\le |\tilde{z}_1|(\|W_1^*\|\|\Phi_1(X_1)\| + \tilde{\epsilon}_1) \\ &\le \frac{\tilde{z}_1^2}{2a_1^2}\theta_1\Phi_1^{\mathrm{T}}(X_1)\Phi_1(X_1) \\ &\quad + \frac{a_1^2}{2} + \frac{\tilde{z}_1^2}{2} + \frac{\tilde{\epsilon}_1^2}{2}, \end{aligned} \tag{9}$$

where $a_1 > 0$ is a designed parameter and $X_1 = (x_1, \hat{\theta}_1, \tilde{\chi}_1, y_d, \dot{y}_d)^{\mathrm{T}} \in \mathbb{R}^5$. For the sake of simplicity, $\Phi_1(X_1)$ will be abbreviated as Φ_1 in the following.

Hence, $\dot{V}_1$ can be rewritten as

$$\dot{V}_1 = \frac{1}{2a_1^2}\tilde{z}_1^2\theta_1\Phi_1^{\mathrm{T}}\Phi_1 + \frac{1}{2}\tilde{z}_1^2 + \tilde{z}_1\mathcal{D}^{1-\alpha_1}\chi_1 - \tilde{z}_1\dot{\tilde{\chi}}_1 + \frac{1}{\eta_1}\tilde{\theta}_1\dot{\hat{\theta}}_1 - \lambda_1 z_1\tilde{z}_1 - \bar{\lambda}_1\tilde{z}_1\tilde{\chi}_1^r + \Theta_1,$$

where $\Theta_1 = \frac{1}{2}a_1^2 + \frac{1}{2}\bar{\epsilon}_1^2 + \zeta_1\rho$. Design the intermediate signal $h_1(t)$ and the adaptive law of $\hat{\theta}_1$ as

$$h_1(t) = -\left(\gamma_1 + \frac{1}{2}\right)\frac{\tilde{z}_1}{\kappa_1} - \frac{\tilde{z}_1\hat{\theta}_1}{2a_1^2\kappa_1}\Phi_1^{\mathrm{T}}\Phi_1 - \frac{\bar{\gamma}_1}{\kappa_1}\vartheta_1(\tilde{z}_1), \tag{10}$$

$$\dot{\hat{\theta}}_1 = \frac{\eta_1}{2a_1^2}\tilde{z}_1^2\Phi_1^{\mathrm{T}}\Phi_1 - \mu_1\hat{\theta}_1 - \xi_1\hat{\theta}_1^r, \hat{\theta}_1(0) \geq 0, \tag{11}$$

where $\gamma_1, \bar{\gamma}_1, \mu_1, \xi_1 > 0$ are designed parameters, and

$$\vartheta_1(\tilde{z}_1) = \begin{cases} \tilde{z}_1^r, & |\tilde{z}_1| \geq \tau_1, \\ A_1\tilde{z}_1 - B_1\tilde{z}_1^3, & |\tilde{z}_1| < \tau_1, \end{cases}$$

with $A_1 = \frac{1}{2}(3-r)\tau_1^{r-1}$, $B_1 = \frac{1}{2}\tau_1^{r-3}(1-r)$, and a small constant $\tau_1 > 0$.

Remark 4 Motivated by [32], the term $\tilde{z}_1^r$ is modified to $A_1\tilde{z}_1 - B_1\tilde{z}_1^3$ when $|\tilde{z}_1|$ is less than the small positive constant τ_1. This modification can ensure that: (i) the singularity phenomenon of $\mathcal{D}^{\alpha_1}h_1(t)$ can be avoided when $\tilde{z}_1 = 0$; (ii) $\mathcal{D}^{\alpha_1}h_1(t)$ is continuous function of $(x, \hat{\theta}_1, y_d)^{\mathrm{T}}$.

It follows from (5)–(7), (10) and (11) that

$$\begin{aligned}\dot{V}_1 &\leq \frac{1}{2a_1^2}\tilde{z}_1^2\theta_1\Phi_1^{\mathrm{T}}\Phi_1 + \frac{1}{2}\tilde{z}_1^2 + \kappa_1\tilde{z}_1h_1(t) \\ &\quad + \lambda_1\tilde{z}_1\tilde{\chi}_1 + \frac{1}{\eta_1}\tilde{\theta}_1\dot{\hat{\theta}}_1 - \lambda_1 z_1\tilde{z}_1 + \Theta_1 \\ &= -(\gamma_1 + \lambda_1)\tilde{z}_1^2 - \bar{\gamma}_1\tilde{z}_1\vartheta_1(\tilde{z}_1) \\ &\quad - \frac{\mu_1}{\eta_1}\tilde{\theta}_1\hat{\theta}_1 - \frac{\xi_1}{\eta_1}\tilde{\theta}_1\hat{\theta}_1^r + \Theta_1.\end{aligned}$$

Step i ($2 \leq i \leq n-1$): From (2) and (3), and Lemma 1, one can obtain that

$$\begin{aligned}\dot{z}_i &= \mathcal{D}^{1-\alpha_i}\mathcal{D}^{\alpha_i}x_i - \dot{\chi}_{i-1} \\ &= \mathcal{D}^{1-\alpha_i}\big(z_{i+1} + \chi_i + f_i(x) + \Delta_i(t)\big) - \dot{\chi}_{i-1}.\end{aligned} \tag{12}$$

Since $\mathcal{D}^{1-\alpha_i}\chi_i$ appears in the above equation, we design the following filter to approximate the virtual control signal χ_i

$$\mathcal{D}^{1-\alpha_i}\chi_i(t) = -\kappa_i(\chi_i(t) - h_i(t)), \chi_i(0) = 0, \tag{13}$$

where $\kappa_i > 0$ is a designed parameter and $h_i(t)$ is an intermediate signal that will be designed later. To compensate for the error between χ_i and h_i, we define a compensated signal $\tilde{\chi}_i$ that is determined by

$$\dot{\tilde{\chi}}_i(t) = -\lambda_i\tilde{\chi}_i(t) - \bar{\lambda}_i\tilde{\chi}_i^r(t) - \kappa_i\chi_i(t), \tilde{\chi}_i(0) = z_i(0), \tag{14}$$

where $\lambda_i, \bar{\lambda}_i > 0$ are designed parameters. Let $\tilde{z}_i = z_i - \tilde{\chi}_i$, from (12), we have

$$\dot{\tilde{z}}_i = \mathcal{D}^{1-\alpha_i}\big(z_{i+1} + \chi_i + f_i(x) + \Delta_i(t)\big) - \dot{\chi}_{i-1} - \dot{\tilde{\chi}}_i. \tag{15}$$

Construct the following Lyapunov function

$$V_i = V_{i-1} + \frac{1}{2}\tilde{z}_i^2 + \frac{1}{2\eta_i}\tilde{\theta}_i^2,$$

where η_i is a designed parameter, $\tilde{\theta}_i = \hat{\theta}_i - \theta_i$ is the estimation error of $\theta_i = \|W_i^*\|^2$, $\hat{\theta}_i$ is the estimate of θ_i, and W_i^* is the weight vector that will be defined later. The derivative of V_i can be computed as

$$\dot{V}_i = \dot{V}_{i-1} + \tilde{z}_i\big(\mathcal{D}^{1-\alpha_i}(z_{i+1} + \chi_i + f_i(x) + \Delta_i(t)) - \dot{\chi}_{i-1} - \dot{\tilde{\chi}}_i\big) + \frac{1}{\eta_i}\tilde{\theta}_i\dot{\hat{\theta}}_i.$$

From Assumption 1, these exists a constant $d_i > 0$ such that $|\mathcal{D}^{1-\alpha_i}\Delta_i(t)| \leq d_i$, which, together with Lemma 2, implies that

$$\tilde{z}_i\mathcal{D}^{1-\alpha_i}\Delta_i(t) \leq d_i|\tilde{z}_i| \leq d_i\tilde{z}_i\tanh\left(\frac{d_i\tilde{z}_i}{\zeta_i}\right) + \zeta_i\rho.$$

Therefore, we have

$$\begin{aligned}\dot{V}_i &\leq \dot{V}_{i-1} + \tilde{z}_i\mathcal{H}_i(Z_i) + \tilde{z}_i\mathcal{D}^{1-\alpha_i}\chi_i - \tilde{z}_i\dot{\tilde{\chi}}_i \\ &\quad + \frac{1}{\eta_i}\tilde{\theta}_i\dot{\hat{\theta}}_i + \zeta_i\rho - \lambda_i z_i\tilde{z}_i - \bar{\lambda}_i\tilde{z}_i\tilde{\chi}_i^r,\end{aligned} \tag{16}$$

where $\mathcal{H}_i(Z_i) = \mathcal{D}^{1-\alpha_i}(z_{i+1} + f_i(x)) + d_i\tanh\left(\frac{d_i\tilde{z}_i}{\zeta_i}\right) - \dot{\chi}_{i-1} + \lambda_i z_i + \bar{\lambda}_i\tilde{\chi}_i^r$ with $Z_i = (x^{\mathrm{T}}, \hat{\theta}_1, \ldots, \hat{\theta}_i, \tilde{\chi}_i, y_d, \dot{y}_d)^{\mathrm{T}} \in \mathbb{R}^{n+i+3}$. Similar to the statement in Step 1, the continuity of $\mathcal{D}^{1-\alpha_i}(z_{i+1} + f_i(x))$ can be obtained. Besides, according to the fractional-order filter (5) and (13), $\mathcal{D}^{1-\alpha_{i-1}}\chi_{i-1}$ must exist, which, together with Definition 1, implies that $\dot{\chi}_{i-1}$ is continuous. Based on Lemma 6, continuous function $\mathcal{H}_i(Z_i)$ can be approximated as

$$\mathcal{H}_i(Z_i) = W_i^{*T}\Phi_i(Z_i) + \epsilon_i(Z_i),$$

where W_i^* denotes the ideal weight and $\epsilon_i(Z_i)$ is the approximation error satisfying $|\epsilon_i(Z_i)| < \tilde{\epsilon}_i$ with positive constant $\tilde{\epsilon}_i$. According to Lemma 7 and using the same manner as in (9), we have

$$\tilde{z}_i\mathcal{H}_i(Z_i) \le \frac{1}{2a_i^2}\tilde{z}_i^2\theta_i\Phi_i^{\mathrm{T}}(X_i)\Phi_i(X_i) + \frac{1}{2}a_i^2 + \frac{1}{2}\tilde{z}_i^2 + \frac{1}{2}\tilde{\epsilon}_i^2,$$

where $a_i > 0$ is a designed parameter and $X_i = (x_1, \ldots, x_i, \hat{\theta}_1, \ldots, \hat{\theta}_i, \tilde{\chi}_i, y_d, \dot{y}_d)^{\mathrm{T}} \in \mathbb{R}^{2i+3}$. For convenience, argument X_i in $\Phi_i(X_i)$ will be omitted in the following. Thus, (16) can be rewritten as

$$\dot{V}_i \le \dot{V}_{i-1} + \frac{1}{2a_i^2}\tilde{z}_i^2\theta_i\Phi_i^{\mathrm{T}}\Phi_i + \frac{1}{2}\tilde{z}_i^2 + \tilde{z}_i\mathcal{D}^{1-\alpha_i}\chi_i - \tilde{z}_i\dot{\tilde{\chi}}_i + \frac{1}{\eta_i}\tilde{\theta}_i\dot{\hat{\theta}}_i - \lambda_i z_i\tilde{z}_i - \bar{\lambda}_i\tilde{z}_i\tilde{\chi}_i^r + \frac{1}{2}a_i^2 + \frac{1}{2}\tilde{\epsilon}_i^2 + \zeta_i\rho,$$

The intermediate signal $h_i(t)$ and the adaptive law of $\hat{\theta}_i$ are designed as

$$h_i(t) = -\left(\gamma_i + \frac{1}{2}\right)\frac{\tilde{z}_i}{\kappa_i} - \frac{\tilde{z}_i\hat{\theta}_i}{2a_i^2\kappa_i}\Phi_i^{\mathrm{T}}\Phi_i - \frac{\bar{\gamma}_i}{\kappa_i}\vartheta_i(\tilde{z}_i), \tag{17}$$

$$\dot{\hat{\theta}}_i = \frac{\eta_i}{2a_i^2}\tilde{z}_i^2\Phi_i^{\mathrm{T}}\Phi_i - \mu_i\hat{\theta}_i - \xi_i\hat{\theta}_i^r, \hat{\theta}_i(0) \ge 0, \tag{18}$$

where $\gamma_i, \bar{\gamma}_i, \mu_i, \xi_i > 0$ are designed parameters, and

$$\vartheta_i(\tilde{z}_i) = \begin{cases} \tilde{z}_i^r, & |\tilde{z}_i| \ge \tau_i, \\ A_i\tilde{z}_i - B_i\tilde{z}_i^3, & |\tilde{z}_i| < \tau_i, \end{cases}$$

with $A_i = \frac{1}{2}(3-r)\tau_i^{r-1}$, $B_i = \frac{1}{2}\tau_i^{r-3}(1-r)$, and a small constant $\tau_i > 0$. Substituting (13), (14), (17) and (18) into $\dot{V}_i$, we have

$$\begin{aligned}\dot{V}_i &\le \dot{V}_{i-1} + \frac{1}{2a_i^2}\tilde{z}_i^2\theta_i\Phi_i^{\mathrm{T}}\Phi_i + \frac{1}{2}\tilde{z}_i^2 + \kappa_i\tilde{z}_i h_i(t) \\ &\quad + \lambda_i\tilde{z}_i\tilde{\chi}_i + \frac{1}{\eta_i}\tilde{\theta}_i\dot{\hat{\theta}}_i - \lambda_i z_i\tilde{z}_i + \frac{1}{2}a_i^2 + \frac{1}{2}\tilde{\epsilon}_i^2 + \zeta_i\rho \\ &= \dot{V}_{i-1} - (\gamma_i + \lambda_i)\tilde{z}_i^2 - \bar{\gamma}_i\tilde{z}_i\vartheta_i(\tilde{z}_i) - \frac{\mu_i}{\eta_i}\tilde{\theta}_i\hat{\theta}_i \\ &\quad - \frac{\xi_i}{\eta_i}\tilde{\theta}_i\hat{\theta}_i^r + \frac{1}{2}a_i^2 + \frac{1}{2}\tilde{\epsilon}_i^2 + \zeta_i\rho \\ &\le -\sum_{s=1}^{i}\left((\gamma_s + \lambda_s)\tilde{z}_s^2 + \bar{\gamma}_s\tilde{z}_s\vartheta_s(\tilde{z}_s) + \frac{\mu_s}{\eta_s}\tilde{\theta}_s\hat{\theta}_s + \frac{\xi_s}{\eta_s}\tilde{\theta}_s\hat{\theta}_s^r\right) + \Theta_i,\end{aligned}$$

where $\Theta_i = \Theta_{i-1} + \frac{1}{2}a_i^2 + \frac{1}{2}\tilde{\epsilon}_i^2 + \zeta_i\rho$.

Step n: Let the final control signal $u(t)$ be given by the filter

$$\mathcal{D}^{1-\alpha_n}u(t) = -\kappa_n(u(t) - h_n(t)), \quad u(0) = 0, \tag{19}$$

where $\kappa_n > 0$ is a designed parameter and $h_n(t)$ is a intermediate signal that will be specified later. As pointed out in 1-th step, the error between $u(t)$ and $h_n(t)$ cannot be overlooked. Therefore, we design a compensated signal $\tilde{\chi}_n$ to eliminate this error, which is given by

$$\dot{\tilde{\chi}}_n(t) = -\lambda_n\tilde{\chi}_n(t) - \bar{\lambda}_n\tilde{\chi}_n^r(t) - \kappa_n u(t), \ \tilde{\chi}_n(0) = z_n(0), \tag{20}$$

where $\lambda_n, \bar{\lambda}_n > 0$ are designed parameters. Let $\tilde{z}_n = z_n - \tilde{\chi}_n$. Then, by using Lemma 1, we have

$$\begin{aligned}\dot{\tilde{z}}_n &= \mathcal{D}^{1-\alpha_n}\mathcal{D}_n^{\alpha_n}x_n - \dot{\chi}_{n-1} - \dot{\tilde{\chi}}_n \\ &= \mathcal{D}^{1-\alpha_n}\big(u + f_n(x) + \Delta_n(t)\big) - \dot{\chi}_{n-1} - \dot{\tilde{\chi}}_n.\end{aligned} \tag{21}$$

Define the Lyapunov function V_n as follows

$$V_n = V_{n-1} + \frac{1}{2}\tilde{z}_n^2 + \frac{1}{2\eta_n}\tilde{\theta}_n^2,$$

where $\eta_n > 0$ is a designed parameter, $\tilde{\theta}_n = \hat{\theta}_n - \theta_n$ is the estimation error of $\theta_n = \|W_n^*\|^2$, $\hat{\theta}_n$ is the estimate of θ_n, and W_n^* will be defined later. From (21), we obtain

$$\dot{V}_n = \dot{V}_{n-1} + \tilde{z}_n\big(\mathcal{D}^{1-\alpha_n}\big(u + f_n(x) + \Delta_n(t)\big) - \dot{\chi}_{n-1} - \dot{\tilde{\chi}}_n\big) + \frac{1}{\eta_n}\tilde{\theta}_n\dot{\hat{\theta}}_n.$$

Based on Assumption 1, there exists a constant $d_n > 0$ such that $|\mathcal{D}^{1-\alpha_n}\Delta_n(t)| \le d_n$. So, by using Lemma 2, we have

$$\tilde{z}_n\mathcal{D}^{1-\alpha_n}\Delta_n(t) \le d_n|\tilde{z}_n| \le d_n\tilde{z}_n\tanh\left(\frac{d_n\tilde{z}_n}{\zeta_n}\right) + \zeta_n\rho.$$

Therefore, $\dot{V}_n$ becomes

$$\dot{V}_n \le \dot{V}_{n-1} + \tilde{z}_n\mathcal{H}_n(Z_n) + \tilde{z}_n\mathcal{D}^{1-\alpha_n}u - \tilde{z}_n\dot{\tilde{\chi}}_n + \frac{1}{\eta_n}\tilde{\theta}_n\dot{\hat{\theta}}_n + \zeta_n\rho - \lambda_n z_n\tilde{z}_n - \bar{\lambda}_n\tilde{z}_n\tilde{\chi}_n^r, \tag{22}$$

where $\mathcal{H}_n(Z_n) = \mathcal{D}^{1-\alpha_n}f_n(x) + d_n\tanh\left(\frac{d_n\tilde{z}_n}{\zeta_n}\right) + \dot{\chi}_{n-1} + \lambda_n z_n + \bar{\lambda}_n\tilde{\chi}_n^r$ with $Z_n = (x^{\mathrm{T}}, \hat{\theta}_1, \ldots, \hat{\theta}_n, \tilde{\chi}_n, y_d, \dot{y}_d)^{\mathrm{T}} \in \mathbb{R}^{2n+3}$. From Lemma 6, function $\mathcal{H}_n(Z_n)$ is approximated as

$$\mathcal{H}_n(Z_n) = W_n^{*T}\Phi_n(Z_n) + \epsilon_n(Z_n),$$

where W_n^* is the ideal weight vector and $\epsilon_n(Z_n)$ is the approximation error satisfying $|\epsilon_n(Z_n)| < \tilde{\epsilon}_n$. According to Lemma 7 and using the same manner as in (9), we have

$$\tilde{z}_n\mathcal{H}_n(Z_n) \le \frac{1}{2a_n^2}\tilde{z}_n^2\theta_n\Phi_n^{\mathrm{T}}(X_n)\Phi_n(X_n) + \frac{1}{2}a_n^2 + \frac{1}{2}\tilde{z}_n^2 + \frac{1}{2}\tilde{\epsilon}_n^2,$$

where $a_n > 0$ is a designed parameter and $X_n = (x^{\mathrm{T}}, \hat{\theta}_1, \ldots, \hat{\theta}_n, \tilde{\chi}_n, y_d, \dot{y}_d)^{\mathrm{T}} \in \mathbb{R}^{2n+3}$. For simplicity, $\Phi_n(X_n)$ will be abbreviated as Φ_n in the following. Substituting the above inequality into (22), we get

$$\dot{V}_n \le \dot{V}_{n-1} + \frac{1}{2a_n^2}\tilde{z}_n^2\theta_n\Phi_n^{\mathrm{T}}\Phi_n + \frac{1}{2}\tilde{z}_n^2 + \tilde{z}_n\mathcal{D}^{1-\alpha_n}u - \tilde{z}_n\dot{\tilde{\chi}}_n + \frac{1}{\eta_n}\tilde{\theta}_n\dot{\hat{\theta}}_n - \lambda_n z_n\tilde{z}_n - \bar{\lambda}_n\tilde{z}_n\tilde{\chi}_n^r + \frac{1}{2}a_n^2 + \frac{1}{2}\tilde{\epsilon}_n^2 + \zeta_n\rho.$$

The intermediate signal $h_n(t)$ and the adaptive laws of $\hat{\theta}_n$ are designed as

$$h_n(t) = -(\gamma_n + \frac{1}{2})\frac{\tilde{z}_n}{\kappa_n} - \frac{\tilde{z}_n\hat{\theta}_n}{2a_n^2\kappa_n}\Phi_n^{\mathrm{T}}\Phi_n - \frac{\bar{\gamma}_n}{\kappa_n}\vartheta_n(\tilde{z}_n), \tag{23}$$

$$\dot{\hat{\theta}}_n = \frac{\eta_n}{2a_n^2}\tilde{z}_n^2\Phi_n^{\mathrm{T}}\Phi_n - \mu_n\hat{\theta}_n - \xi_n\hat{\theta}_n^r, \hat{\theta}_n(0) \ge 0, \tag{24}$$

where $\gamma_n, \bar{\gamma}_n, \mu_n, \xi_n > 0$ are designed parameters and

$$\vartheta_n(\tilde{z}_n) = \begin{cases} \tilde{z}_n^r, & |\tilde{z}_n| \ge \tau_n, \\ A_n\tilde{z}_n - B_n\tilde{z}_n^3, & |\tilde{z}_n| < \tau_n, \end{cases}$$

with $A_n = \frac{1}{2}(3-r)\tau_n^{r-1}$, $B_n = \frac{1}{2}\tau_n^{r-3}(1-r)$, and a small constant $\tau_n > 0$. Taking (19), (20), (23) and (24) into $\dot{V}_n$, one has

$$\begin{aligned}\dot{V}_n &\le \dot{V}_{n-1} + \frac{1}{2a_n^2}\tilde{z}_n^2\theta_n\Phi_n^{\mathrm{T}}\Phi_n + \frac{1}{2}\tilde{z}_n^2 + \kappa_n\tilde{z}_n h_n(t) \\ &\quad + \lambda_n\tilde{z}_n\tilde{\chi}_n + \frac{1}{\eta_n}\tilde{\theta}_n\dot{\hat{\theta}}_n - \lambda_n z_n\tilde{z}_n \\ &\quad + \frac{1}{2}a_n^2 + \frac{1}{2}\tilde{\epsilon}_n^2 + \zeta_n\rho \\ &\le -\sum_{s=1}^{n}\left((\gamma_s + \lambda_s)\tilde{z}_s^2 + \bar{\gamma}_s\tilde{z}_s\vartheta_s(\tilde{z}_s) + \frac{\mu_s}{\eta_s}\tilde{\theta}_s\hat{\theta}_s + \frac{\xi_s}{\eta_s}\tilde{\theta}_s\hat{\theta}_s^r\right) + \Theta_n, \end{aligned} \tag{25}$$

where $\Theta_n = \Theta_{n-1} + \frac{1}{2}a_n^2 + \frac{1}{2}\tilde{\epsilon}_n^2 + \zeta_n\rho = \sum_{s=1}^{n}(\frac{1}{2}a_s^2 + \frac{1}{2}\tilde{\epsilon}_s^2 + \zeta_s\rho)$.

Before giving the main result of this paper, we give two useful lemmas.

Lemma 8 *For the filters (5), (13) and (19), if the signal $h_i(t)$ $(1 \le i \le n)$ is bounded, then signals $\tilde{h}_i(t) = \chi_i(t) - h_i(t)$ $(1 \le i \le n-1)$, $\tilde{h}_n(t) = u(t) - h_n(t)$, $\chi_i(t)$ $(1 \le i \le n-1)$ and $u(t)$ are bounded for $t \ge 0$.*

Proof For the sake of simplicity, $u(t)$ is denoted by $\chi_n(t)$, so $\tilde{h}_n(t) = \chi_n(t) - h_n(t)$. Since $h_i(t)$ $(1 \le i \le n)$ is bounded, there exists a positive constant $\bar{h}_i$ such that $|h_i(t)| \le \bar{h}_i$. Considering the Lyapunov function $V_{\chi_i}(t) = \frac{1}{2}\chi_i^2(t)$, we have

$$\begin{aligned}\mathcal{D}^{1-\alpha_i}V_{\chi_i}(t) &\le \chi_i(t)\mathcal{D}^{1-\alpha_i}\chi_i(t) \\ &= -\kappa_i\chi_i^2(t) + \kappa_i\chi_i(t)h_i(t).\end{aligned}$$

It follows from $|h_i(t)| \le \bar{h}_i$ that $\chi_i(t)h_i(t) \le \frac{1}{2}\chi_i^2(t) + \frac{1}{2}h_i^2(t) \le \frac{1}{2}\chi_i^2(t) + \frac{1}{2}\bar{h}_i^2$, which means

$$\begin{aligned}\mathcal{D}^{1-\alpha_i}V_{\chi_i}(t) &\le -\frac{1}{2}\kappa_i\chi_i^2(t) + \frac{1}{2}\kappa_i\bar{h}_i^2 \\ &= -\kappa_i V_{\chi_i}(t) + \frac{1}{2}\kappa_i\bar{h}_i^2.\end{aligned}$$

Therefore, from $0 \le E_{1-\alpha_i}(-\kappa_i t^{1-\alpha_i}) < 1$ for $t \ge 0$ and Lemma 5 in [42], we have

$$\begin{aligned}V_{\chi_i}(t) &\le \left(V_{\chi_i}(0) - \frac{1}{2}\bar{h}_i^2\right)E_{1-\alpha_i}(-\kappa_i t^{1-\alpha_i}) + \frac{1}{2}\bar{h}_i^2 \\ &\le V_{\chi_i}(0) + \frac{1}{2}\bar{h}_i^2,\end{aligned}$$

from which we can obtain that $\chi_i^2(t) \le \chi_i^2(0) + \bar{h}_i^2$ for $t \ge 0$. That is, $\chi_i(t)$ $(1 \le i \le n)$ is bounded. From the boundedness of $\chi_i(t)$ and $h_i(t)$, it is obvious that $\tilde{h}_i(t)$ is bounded. This completes the proof. □

Lemma 9 *For the compensated filters (6), (14) and (20), if signals χ_i $(1 \le i \le n-1)$ and $u(t)$ are bounded, then signal $\tilde{\chi} = (\tilde{\chi}_1, \ldots, \tilde{\chi}_n)^{\mathrm{T}}$ converges to a small region $\Omega_1 = \{\tilde{\chi} \mid \|\tilde{\chi}\|^2 \le 2\omega_1\}$ in finite-time T_1, where $T_1 = T_1(\bar{q}_1, \bar{q}_2, \bar{q}_3)$ is determined by (1), $\bar{q}_1, \bar{q}_2, \bar{q}_3 > 0$ will be given in the following, and*

$$\omega_1 = \min\left\{\frac{\bar{q}_3}{(1-\varrho)\bar{q}_1}, \left(\frac{\bar{q}_3}{(1-\varrho)\bar{q}_2}\right)^{\frac{2}{1+r}}\right\}.$$

Proof For convenience, $u(t)$ is denoted by $\chi_n(t)$. Defining the Lyapunov function $V_{\tilde{\chi}}(t) = \frac{1}{2}\sum_{s=1}^{n}\tilde{\chi}_s^2$, and noting (6), (14) and (20), we have

$$\dot{V}_{\tilde{\chi}}(t) = \sum_{s=1}^{n}\tilde{\chi}_s\dot{\tilde{\chi}}_s = -\sum_{s=1}^{n}\left(\lambda_s\tilde{\chi}_s^2 + \bar{\lambda}_s\tilde{\chi}_s^{1+r}\right) - \sum_{s=1}^{n}\kappa_s\tilde{\chi}_s\chi_s.$$

By using the Young's inequality, we obtain

$$-\tilde{\chi}_s\chi_s \le |\tilde{\chi}_s\chi_s| \le \frac{\lambda_s}{2\kappa_s}\tilde{\chi}_s^2 + \frac{\kappa_s}{2\lambda_s}\chi_s^2.$$

Because χ_s is bounded, there is a constant $\bar{\bar{\Theta}}_s > 0$ such that $\frac{\kappa_s^2}{2\lambda_s}\chi_s^2 \le \bar{\bar{\Theta}}_s$. Thus, $-\kappa_s\tilde{\chi}_s\chi_s \le \frac{1}{2}\lambda_s\tilde{\chi}_s^2 + \bar{\bar{\Theta}}_s$. By using Lemma 4, $\dot{V}_{\tilde{\chi}}(t)$ can be rewritten as

$$\begin{aligned}\dot{V}_{\tilde{\chi}}(t) &\le -\sum_{s=1}^{n}\left(\frac{1}{2}\lambda_s\tilde{\chi}_s^2 + \bar{\lambda}_s\tilde{\chi}_s^{1+r}\right) + \sum_{s=1}^{n}\bar{\bar{\Theta}}_s \\ &\le -\bar{q}_1 V_{\tilde{\chi}}(t) - \bar{q}_2 V_{\tilde{\chi}}^{\frac{1+r}{2}}(t) + \bar{q}_3,\end{aligned} \tag{26}$$

where $\bar{q}_1 = \min\{\lambda_s, s = 1,\ldots,n\}$, $\bar{q}_2 = 2^{\frac{1+r}{2}}\min\{\bar{\lambda}_s, s = 1,\ldots,n\}$ and $\bar{q}_3 = \sum_{s=1}^{n}\bar{\bar{\Theta}}_s$. It then follows from Lemma 5 that $\tilde{\chi} = (\tilde{\chi}_1,\ldots,\tilde{\chi}_n)^{\mathrm{T}}$ converges to Ω_1 in finite-time T_1. The proof is completed. □

Eventually, the practical finite-time adaptive neural networks control schemes and the parameter adaptive laws are designed, from which we establish the main result of this paper.

Theorem 1 *For incommensurate fractional-order nonlinear system* (2) *under Assumptions* 1–3, *the designed virtual control signals determined by* (5), (13), *final control signal determined by* (19), *adaptive laws* (11), (18), (24), *intermediate signals* (10), (17), (23), *and compensated signals determined by* (6), (14), (20) *can ensure that:*

(i) *all signals in the closed-loop system are bounded;*
(ii) *the signal* $\tilde{z} = (\tilde{z}_1,\ldots,\tilde{z}_n)^{\mathrm{T}}$ *converges to a small region* $\Omega_2 = \left\{\tilde{z}\,|\,\|\tilde{z}\|^2 \le 2\omega_2\right\}$ *in finite-time* T_2, *and the signal* $z = (z_1,\ldots,z_n)^{\mathrm{T}}$ *converges to* $\Omega_3 = \left\{z\,|\,\|z\|^2 \le 4\omega_3\right\}$ *in finite-time* T,

where $T = \max\{T_1, T_2\}$, $T_1 = T_1(\bar{q}_1,\bar{q}_2,\bar{q}_3)$ *and* $T_2 = T_2(q_1,q_2,q_3)$ *are determined by* (1), q_1, q_2, q_3 *will be specified later,* $\bar{q}_1,\bar{q}_2,\bar{q}_3 > 0$ *are given in Lemma* 9, *and* $\omega_3 = \omega_1 + \omega_2$,

$$\omega_2 = \min\left\{\frac{q_3}{(1-\varrho)q_1}, \left(\frac{q_3}{(1-\varrho)q_2}\right)^{\frac{2}{1+r}}\right\}.$$

Proof For convenience, let $\mathbb{S} = \{s|s = 1,\ldots,n\}$, $\mathbb{S}_1 = \{s \in \mathbb{S}||\tilde{z}_s| < \tau_s\}$ and $\mathbb{S}_2 = \{s \in \mathbb{S}||\tilde{z}_s| \ge \tau_s\}$. By using Lemma 3 and noting that $r = \frac{r_1}{r_2} \in (0,1)$ with positive odd numbers r_1, r_2, for $s \in \mathbb{S}$, we have

$$-\tilde{\theta}_s\hat{\theta}_s^r = \tilde{\theta}_s(-\hat{\theta}_s)^r \le -b_1\tilde{\theta}_s^{1+r} + b_2\theta_s^{1+r}, \tag{27}$$

where $b_1, b_2 > 0$ are given in Lemma 3. Consider the Lyapunov function

$$V_n(\Upsilon(t)) = \sum_{s\in\mathbb{S}}\left(\frac{1}{2}\tilde{z}_s^2 + \frac{1}{2\eta_s}\tilde{\theta}_s^2\right), \tag{28}$$

where $\Upsilon(t) = (\tilde{z}_1,\ldots,\tilde{z}_n,\tilde{\theta}_1,\ldots,\tilde{\theta}_n)^{\mathrm{T}}$. Then, from (25), (27) and the inequality $-\tilde{\theta}_s\hat{\theta}_s = -\tilde{\theta}_s^2 - \tilde{\theta}_s\theta_s \le -\frac{1}{2}\tilde{\theta}_s^2 + \frac{1}{2}\theta_s^2$, we have

$$\begin{aligned}\dot{V}_n \le -\sum_{s\in\mathbb{S}}\Bigg((\gamma_s+\lambda_s)\tilde{z}_s^2 + \bar{\gamma}_s\tilde{z}_s\vartheta_s(\tilde{z}_s) + \frac{\mu_s}{2\eta_s}\tilde{\theta}_s^2 \\ + \frac{b_1\xi_s}{\eta_s}\tilde{\theta}_s^{1+r}\Bigg) + \bar{\Theta}_1,\end{aligned} \tag{29}$$

where $\bar{\Theta}_1 = \Theta_n + \sum_{s\in\mathbb{S}}\left(\frac{\mu_s}{2\eta_s}\theta_s^2 + \frac{b_2\xi_s}{\eta_s}\theta_s^{1+r}\right)$. According to the form of $\vartheta_s(\tilde{z}_s)$, we can obtain that

$$\begin{aligned}&-\sum_{s\in\mathbb{S}}\bar{\gamma}_s\tilde{z}_s\vartheta_s(\tilde{z}_s) \\ &= -\sum_{s\in\mathbb{S}_1}\bar{\gamma}_s A_s\tilde{z}_s^2 - \sum_{s\in\mathbb{S}_2}\bar{\gamma}_s\tilde{z}_s^{1+r} + \sum_{s\in\mathbb{S}_1}\bar{\gamma}_s B_s\tilde{z}_s^4 \\ &\le -\sum_{s\in\mathbb{S}_1}\bar{\gamma}_s A_s\tilde{z}_s^2 - \sum_{s\in\mathbb{S}}\bar{\gamma}_s\tilde{z}_s^{1+r} + \bar{\Theta}_2,\end{aligned}$$

where $\bar{\Theta}_2 = \sum_{s\in\mathbb{S}_1}\bar{\gamma}_s(B_s\tau_s^4 + \tau_s^{1+r})$. Therefore, by using Lemma 4, (29) becomes

$$\begin{aligned}\dot{V}_n \le\ & -\sum_{s\in\mathbb{S}_1}(\bar{\gamma}_s A_s + \gamma_s + \lambda_s)\tilde{z}_s^2 - \sum_{s\in\mathbb{S}_2}(\gamma_s+\lambda_s)\tilde{z}_s^2 \\ & -\sum_{s\in\mathbb{S}}\left(\bar{\gamma}_s\tilde{z}_s^{1+r} + \frac{\mu_s}{2\eta_s}\tilde{\theta}_s^2 + \frac{b_1\xi_s}{\eta_s}\tilde{\theta}_s^{1+r}\right) + \bar{\Theta}_1 + \bar{\Theta}_2 \\ \le\ & -q_1 V_n - q_2\sum_{s\in\mathbb{S}}\left(\left(\frac{1}{2}\tilde{z}_s^2\right)^{\frac{1+r}{2}} + \left(\frac{1}{2\eta_s}\tilde{\theta}_s^2\right)^{\frac{1+r}{2}}\right) + q_3 \\ \le\ & -q_1 V_n - q_2\left(\sum_{s\in\mathbb{S}}\left(\frac{1}{2}\tilde{z}_s^2 + \frac{1}{2\eta_s}\tilde{\theta}_s^2\right)\right)^{\frac{1+r}{2}} + q_3 \\ \le\ & -q_1 V_n - q_2 V_n^{\frac{1+r}{2}} + q_3,\end{aligned} \tag{30}$$

where $q_1 = \min\{2\min_{s\in\mathbb{S}_1}\{\bar{\gamma}_s A_s + \gamma_s + \lambda_s\}, 2\min_{s\in\mathbb{S}_2}\{\gamma_s + \lambda_s\}, \min_{s\in\mathbb{S}}\{\mu_s\}\}$, $q_2 = 2^{\frac{1+r}{2}} \min_{s\in\mathbb{S}}\{\bar{\gamma}_s, b_1\xi_s\eta_s^{\frac{1+r}{2}}\}$ and $q_3 = \bar{\Theta}_1 + \bar{\Theta}_2$.

(i) Since V_n is positive definite, from (28) and (30), we have $\dot{V}_n \le -q_1 V_n + q_3$, which means that

$$V_n = V_n(\Upsilon(t)) \le (V_n(\Upsilon(0)) - \frac{q_3}{q_1})e^{-q_1 t} + \frac{q_3}{q_1} \le V_n(\Upsilon(0)) + \frac{q_3}{q_1}.$$

Thus, $\tilde{z}_i, \tilde{\theta}_i$ $(i = 1, \ldots, n)$ are bounded. Since θ_i is a constant, $\hat{\theta}_i = \tilde{\theta}_i + \theta_i$ is bounded, which means h_i in (10), (17) and (23) is bounded. Based on the boundedness of h_i and Lemma 8, χ_i $(i = 1, \ldots, n-1)$ and u are bounded. Further, the boundedness of $\tilde{\chi}_i$ can be obtained by using Lemma 9, from which we get that $z_i = \tilde{z}_i + \tilde{\chi}_i$ is bounded. According to coordinate transform (3) and Assumption 2, we obtain the boundedness of x_i. Therefore, all signals in the closed-loop system are bounded.

(ii) It follows from Lemma 5 and (30) that there exists a finite-time $T_2 = T_2(q_1, q_2, q_3) > 0$ such that $\tilde{z} = (\tilde{z}_1, \ldots, \tilde{z}_n)^{\mathrm{T}}$ enters Ω_2 for $t \ge T_2$. Noting that $z_i = \tilde{z}_i + \tilde{\chi}_i$ and using Lemma 9, $\|z\|^2 \le 2\|\tilde{z}\|^2 + 2\|\tilde{\chi}\|^2 \le 4(\omega_1 + \omega_2) = 4\omega_3$, i.e., $z \in \Omega_3$ for $t \ge T = \max\{T_1, T_2\}$, where T_1 is given in Lemma 9.

This completes the proof. □

Remark 5 In some previous literature concerning finite-time control of FOS, the formula $\mathcal{D}^\alpha g^\iota(t) = \frac{\Gamma(1+\iota)}{\Gamma(1+\iota-\alpha)} g^{\iota-\alpha}(t)\mathcal{D}^\alpha g(t)$ $(\iota \in \mathbb{R}, \alpha \in (0,1))$ plays a key role in stability analysis. Unfortunately, as pointed out in [4], this formula may not feasible (a counterexample was given in [4]), with the result that the design of a (practical) finite-time adaptive control scheme is quite difficult, because the condition of the fractional-order version (i.e., $\mathcal{D}^\alpha V \le -q_1 V(x) - q_2 V^\iota + q_3$) does not imply the practical finite-time stability of FOS. However, in this paper, with the help of Lemma 1, the first-order derivative of the Lyapunov function is calculated instead of its fractional-order derivative, and thus, the practical finite-time stability of FOS is obtained based on the integer-order condition $\dot{V} \le -q_1 V(x) - q_2 V^\iota + q_3$ (see Lemma 5). According to Lemma 5, a novel and practical finite-time adaptive control scheme is successfully designed for FOS and the stability analysis is also derived.

Remark 6 In order to highlight the proposed novel practical finite-time adaptive control scheme, only a classical incommensurate FOS is considered in this paper. In fact, it is easy to extend the proposed control scheme to cases with more general assumptions, such as systems with unmodeled dynamics, input quantization, unknown control direction, or actuator faults. These systems were considered in [8,19,20,22,37], while the practical finite-time control for these systems remains open.

Remark 7 It can be found that the backstepping method has been successfully applied to the control problem of FOSs in [9,18,19,21,22,37], while these control schemes can only achieve the goal of non-finite time control. In this paper, the practical finite-time control scheme is proposed for incommensurate FOS, which can not only be used for practical finite-time control of commensurate FOS but also be degenerated to the non-finite time control scheme for incommensurate FOS. In addition, the reference signal y_d in this paper is a time-varying function. If $y_d = 0$, then the tracking problem in this paper becomes a stabilization problem.

The following non-finite time control scheme can be obtained from Theorem 1 for an incommensurate fractional-order nonlinear system.

Corollary 1 *Consider the incommensurate fractional-order nonlinear system (2) under Assumptions 1–3, the designed virtual control signals determined by (5), (13), final control signal determined by (19), adaptive laws, intermediate signals and compensated signals determined by* $(i = 1, \ldots, n)$

$$\dot{\hat{\theta}}_i = \frac{\eta_i}{2a_i^2}\tilde{z}_i^2\Phi_i^{\mathrm{T}}\Phi_i - \mu_i\hat{\theta}_i, \tag{31}$$

$$h_i(t) = -\left(\gamma_i + \frac{1}{2}\right)\frac{\tilde{z}_i}{\kappa_i} - \frac{1}{2a_i^2\kappa_i}\tilde{z}_i\hat{\theta}_i\Phi_i^{\mathrm{T}}\Phi_i, \tag{32}$$

$$\dot{\tilde{\chi}}_i(t) = -\lambda_i\tilde{\chi}_i(t) - \kappa_i\chi_i(t), \quad \tilde{\chi}_i(0) = z_i(0), \tag{33}$$

$$\chi_n(t) = u(t), \tag{34}$$

can ensure that: (i) all signals in the closed-loop system are bounded; (ii) the signals $\tilde{z} = (\tilde{z}_1, \ldots, \tilde{z}_n)^{\mathrm{T}}$ *and* $z = (z_1, \ldots, z_n)^{\mathrm{T}}$ *converge to a small regions of origin.*

Proof Let parameters $\bar{\gamma}_i = \bar{\lambda}_i = \xi_i = 0$, then from (6), (10), (11), (14), (17), (18), (20), (23) and (24), we can obtain the forms of adaptive laws, intermediate signals and compensated signals shown in (31)–(34). In addition, consider the same Lyapunov functions $V_n(\Upsilon(t))$ as in Theorem 1 and $V_{\tilde{\chi}}(t)$ as in Lemma 9, the inequalities (26) and 30 will degenerate into

$$\dot{V}_{\tilde{\chi}}(t) \leq -\bar{q}_1 V_{\tilde{\chi}}(t) + \bar{q}_3, \tag{35}$$

$$\dot{V}_n(\Upsilon(t)) \leq -q_1 V_n(\Upsilon(t)) + q_3, \tag{36}$$

where $\bar{q}_1, \bar{q}_3, q_1$ and q_3 are the same as the ones in Lemma 9 and Theorem 1. Then, we can obtain the boundedness of all signals in the closed-loop system by using a similar argument as in the proof of Theorem 1. It follows from (35) and (36) that

$$V_{\tilde{\chi}}(t) \leq \left(V_{\tilde{\chi}}(0) - \frac{\bar{q}_3}{\bar{q}_1}\right)e^{-\bar{q}_1 t} + \frac{\bar{q}_3}{\bar{q}_1},$$

$$V_n(\Upsilon(t))(t) \leq \left(V_n(\Upsilon(0)) - \frac{q_3}{q_1}\right)e^{-q_1 t} + \frac{q_3}{q_1},$$

from which we can only get that signals $\tilde{z}$ and z converge to small regions of origin, and cannot derive the results of finite-time convergence. □

Remark 8 The practical finite-time control scheme proposed in Theorem 1 for FOS (2) contains an adjustable parameter r, which provides a greater degree of freedom in the choice of parameters. Therefore, compared with the non-finite time control scheme in Corollary 1, Theorem 1 gives us a possible option to achieve better control performance.

Remark 9 Compared with the literature [9,18,20–22,36,37], the control scheme in Corollary 1 is also novel and can be used to control both incommensurate and commensurate FOSs in [9,18,20–22,36,37]. The merits of the control scheme in Corollary 1 can be summarized as follows: (i) in contrast to the adaptive laws in [9,20–22], the derivative order of adaptive laws in Corollary 1 is 1, which is easier to implement in practice; (ii) it can be seen from the numerical simulations in some previous studies [18,36,37] that the fluctuation range of control input around the initial time is very large, while in this paper, the control input is generated by the designed filter (19) and such fluctuation of control input can be reduced, which is also illustrated by the numerical simulations in the next section (see Remark 11 for details).

In addition, the form of intermediate signal $h_1(t)$ is similar to the virtual controllers in many literature, but the virtual control signal χ_1 in this paper is generated by fractional filter (5), which is quite different from the form of the virtual control signal in literature. Besides, if system (2) degenerates to integer-order one, then fractional filter (5) becomes $\chi_1(t) = \frac{\kappa_1}{1+\kappa_1}h_1(t)$, and thus, there is only a constant coefficient between $\chi_1(t)$ and control virtual control signal in the literature, which indicates that the virtual control signal is more comprehensive and cover the ones in literature as special cases.

Remark 10 The form of intermediate signals $h_i(t)$ $(i = 1, \ldots, n)$ are similar to the virtual controllers in many literature, but the virtual control signal χ_i in this paper is generated by fractional filters (5), (13) and (19), which are quite different from the form of the virtual control signal in literature. It is worth pointing out that if $\alpha_i = 1$, then the practical finite-time and non-finite time control schemes for FOSs presented in Theorem 1 and Corollary 1 will degenerate to the ones of integer-order nonlinear systems. More precisely, the filters (5), (13) and (19) become $\mathcal{D}^0\chi_i(t) = \chi_i(t) = -\kappa_i(\chi_i(t) - h_i(t))$, i.e., $\chi_i(t) = \frac{\kappa_i}{1+\kappa_i}h_i(t)$. Then substituting $h_i(t)$ into this equation, we have

$$\chi_i(t) = -\frac{1}{1+\kappa_i}\left(\left(\gamma_i + \frac{1}{2}\right)\tilde{z}_i + \frac{1}{2a_i^2}\tilde{z}_i\hat{\theta}_i\Phi_i^{\mathrm{T}}\Phi_i + \bar{\gamma}_i\vartheta_i(\tilde{z}_i)\right).$$

Further, letting $\kappa_i = 0$ in the above equation, one can obtain

$$\chi_i(t) = -\left(\gamma_i + \frac{1}{2}\right)\tilde{z}_i - \frac{1}{2a_i^2}\tilde{z}_i\hat{\theta}_i\Phi_i^{\mathrm{T}}\Phi_i - \bar{\gamma}_i\vartheta_i(\tilde{z}_i),$$

which coincides with the finite-time control scheme in [32,33]. This indicates that the control signals proposed in this paper are more comprehensive and cover the ones in literature as special cases. If we further let $\bar{\gamma}_i = \bar{\lambda}_i = \xi_i = 0$, then the non-finite time control scheme for an integer-order system can be obtained, which was extensively discussed in the existing literature, such as [7,13,15]. Therefore, the proposed control scheme in this paper is more general than the above-mentioned studies.

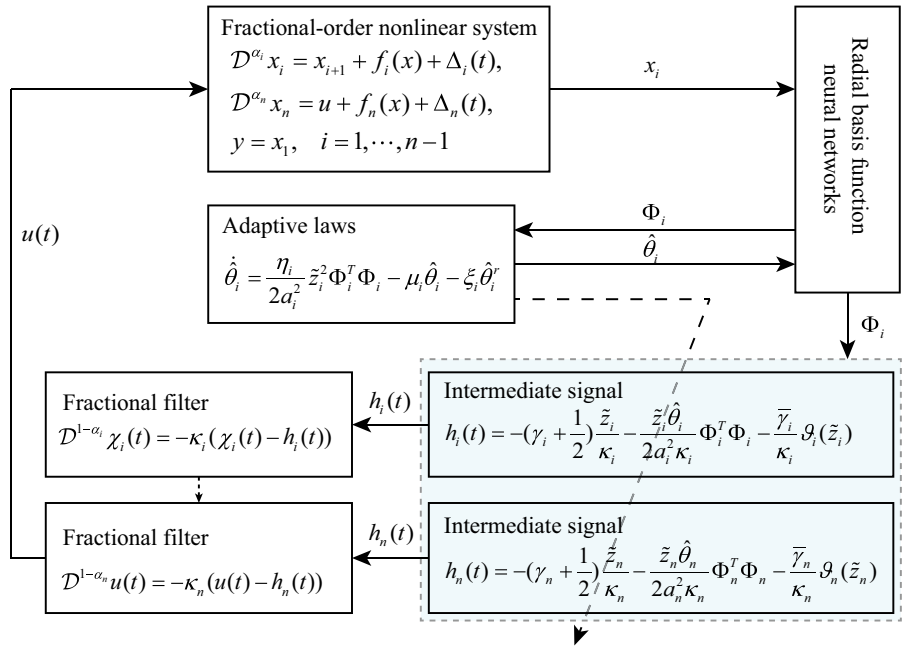

Fig. 1 Block diagram of the closed-loop system

4 Numerical simulations

In this section, two numerical examples are presented to illustrate the effectiveness of the control scheme proposed in the previous section. In order to enhance the readability of this article, a block diagram of the closed-loop system is presented in Fig. 1.

Example 1 Consider the following incommensurate fractional-order nonlinear system

$$\begin{cases} \mathcal{D}^{\alpha_1} x_1 = 2x_2 + 1 - \cos(x_1 x_3) + x_3 + \Delta_1(t), \\ \mathcal{D}^{\alpha_2} x_2 = x_3 + x_2^2 x_3 e^{-x_2^2} + \Delta_2(t), \\ \mathcal{D}^{\alpha_3} x_3 = u + x_1 x_2 e^{-x_3^2} + x_3 \sin(x_1 x_2) + \Delta_3(t), \\ y = x_1, \end{cases} \tag{37}$$

where $\alpha_1 = 0.95$, $\alpha_2 = 0.85$, $\alpha_3 = 0.92$, $\Delta_1(t) = 0.3\cos(0.7t)$, $\Delta_2(t) = -0.1\sin(0.6t)$, $\Delta_3(t) = 0.2\cos(0.8t)$. The reference signal is $y_d = \sin(1.4t) + 0.8\cos(0.7t)$.

It is obvious that y_d, Δ_1, Δ_2, Δ_3 and their derivatives are continuous and bounded. Thus, Assumptions 1 and 2 are satisfied. The designed parameters are chosen as: $r = \frac{5}{9}$, $\gamma_1 = 11.8$, $\gamma_2 = 6.4$, $\gamma_3 = 3.2$, $\bar{\gamma}_1 = 10.76$, $\bar{\gamma}_2 = 4.55$, $\bar{\gamma}_3 = 2.86$, $\lambda_1 = 4.62$, $\lambda_2 = 1.96$, $\lambda_3 = 2.1$, $\bar{\lambda}_1 = 2.9$, $\bar{\lambda}_2 = 1.4$, $\bar{\lambda}_3 = 1.5$, $\kappa_1 = 0.9$, $\kappa_2 = 1.7$, $\kappa_3 = 1.2$, $\eta_1 = 0.2$, $\eta_2 = 0.1$, $\eta_3 = 0.5$, $\mu_1 = 0.003$, $\mu_2 = 0.005$, $\mu_3 = 0.01$, $\xi_1 = 0.001$, $\xi_2 = 0.004$, $\xi_3 = 0.02$, $a_1 = a_2 = 1$, $a_3 = 1.2$, $\tau_1 = \tau_2 = \tau_3 = 0.02$, $\varpi_s = (-4.5, -3, -1.5, 0, 1.5, 3, 4.5)^{\mathrm{T}}$ and $\delta_s = 0.8$. The initial values of the system (37) and the adaptive laws are $x(0) = (-0.1, -0.1, 0.9)^{\mathrm{T}}$, $\hat{\theta}_1(0) = 10^{-6}$, $\hat{\theta}_2(0) = 10^{-4}$ and $\hat{\theta}_3(0) = 10^{-3}$.

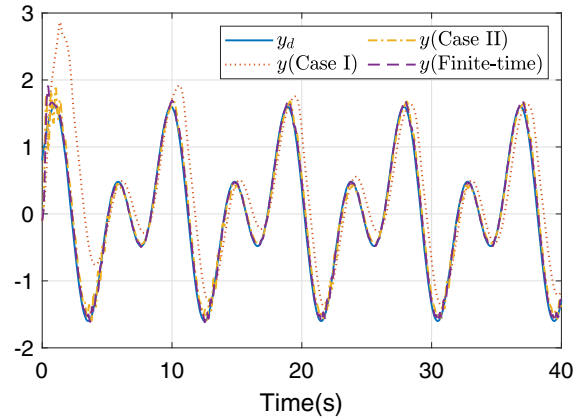

Fig. 2 Trajectories of reference signal y_d and system output y

The simulation results are shown in Figs. 2–7. The system output $y = x_1$ and the tracking error z_1 under the proposed practical finite-time control scheme are given in Figs. 2 and 3, respectively, from which we see that y can track the reference signal y_d with a small tracking error. To compare with the non-finite time con-

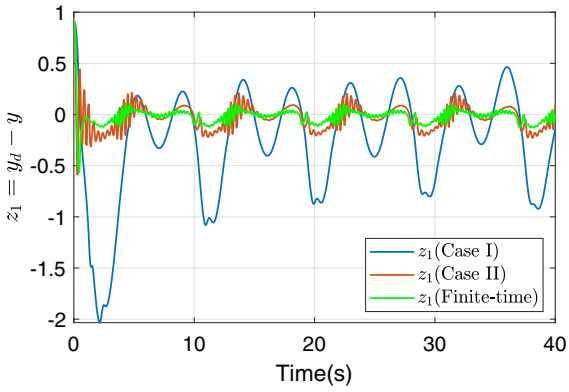

Fig. 3 Trajectories of tracking error $z_1 = y_d - y$

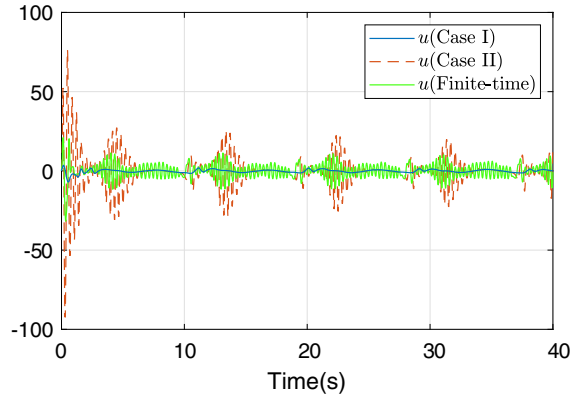

Fig. 4 Trajectories of system input u

trol scheme (i.e., the results in Corollary 1), we also consider the following two cases for Corollary 1: Case I, all parameters are the same as in case of practical finite-time control, except $\bar{\gamma}_i = \bar{\lambda}_i = \xi_i = 0$; Case II, $\gamma_1 = 19.6, \gamma_2 = 11, \gamma_3 = 11.2, \lambda_1 = 11.62, \lambda_2 = 7.56, \lambda_3 = 7.7, \bar{\gamma}_i = \bar{\lambda}_i = \xi_i = 0$ and other parameters are the same as in case of practical finite-time control. We present the trajectories of y and z_1 under the non-finite time control scheme in Figs. 2 and 3, respectively. From Fig. 3, compared with the tracking error under the non-finite time control scheme, the proposed finite-time control scheme has a smaller tracking error and has a slighter oscillation. In addition, from the trajectories of system input u under practical finite-time and non-finite time control schemes shown in Fig. 4, we see that: (i) the tracking performance is very bad in Case I from Fig. 3, although the control force is smaller than that of practical finite-time control; (ii) the fluctuation range of u for practical finite-time control is smaller than that for non-finite time control in Case II, which, together with Fig. 3, means that the proposed practical finite-time control scheme can achieve better tracking performance under a smaller control force compared with the non-finite time control scheme in Case II. The trajectories of state variables x_2 and x_3 are given in Fig. 5. Figure 6 shows the trajectories of adaptive parameters $\hat{\theta}_1, \hat{\theta}_2$ and $\hat{\theta}_3$. Figure 7 gives the trajectories of virtual control signals χ_1, χ_2 and compensated signals $\tilde{\chi}_1, \tilde{\chi}_2, \tilde{\chi}_3$. All figures indicate the boundedness of signals in the proposed practical finite-time control scheme.

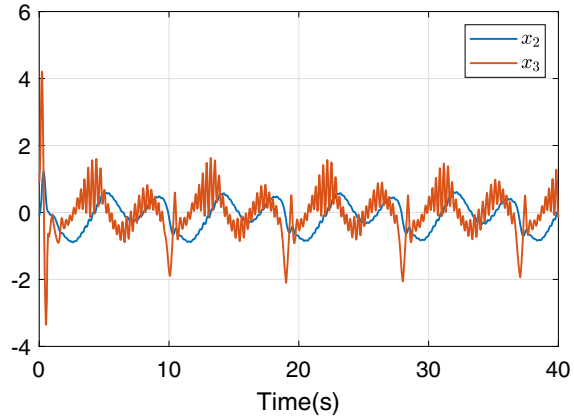

Fig. 5 Trajectories of state variables x_2 and x_3

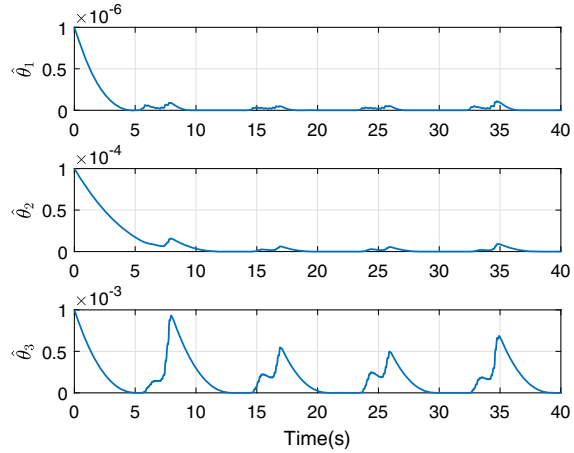

Fig. 6 Trajectories of estimated parameter $\hat{\theta}_i$

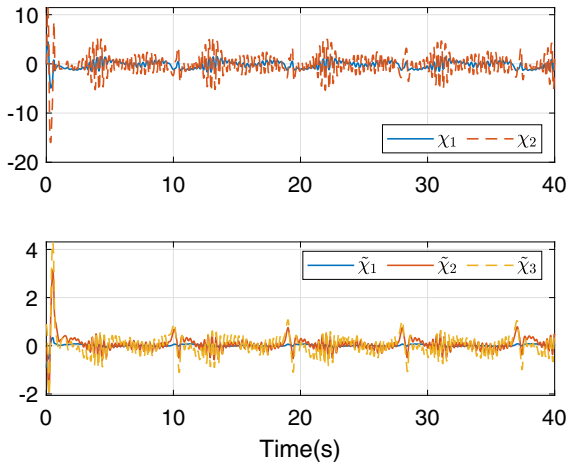

Fig. 7 Trajectories of virtual control signals χ_1, χ_2 and compensated signals $\tilde{\chi}_i$

Example 2 We consider the following fractional-order Chua–Hartley's system [2]

$$\begin{cases} \mathcal{D}^{\alpha_1} x_1 = 10x_2 + \frac{10}{7}(x_1 - x_1^3) + \Delta_1(t), \\ \mathcal{D}^{\alpha_2} x_2 = x_3 + x_1 - x_2 + \Delta_2(t), \\ \mathcal{D}^{\alpha_3} x_3 = u - \frac{100}{7} x_2 + \Delta_3(t), \\ y = x_1, \end{cases} \tag{38}$$

where $\alpha_1 = \alpha_2 = 0.98, \alpha_3 = 0.94$, $\Delta_1(t) = 0.5\sin(0.8t)$, $\Delta_2(t) = 0.4\cos(0.8t)$, $\Delta_3(t) = -0.5\sin(0.8t)$. The reference signal is $y_d = \sin(0.8t) + \cos(0.8t)$.

It follows from the forms of the reference signal and external disturbances that Assumptions 1 and 2 are satisfied. The designed parameters in the practical finite-time control scheme are chosen as: $r = 5/11$, $\gamma_1 = 1.16, \gamma_2 = 13.88, \gamma_3 = 12.84, \bar{\gamma}_1 = 0.66, \bar{\gamma}_2 = 13.7, \bar{\gamma}_3 = 4.36, \lambda_1 = 3.02, \lambda_2 = 5.78, \lambda_3 = 2.42, \bar{\lambda}_1 = 1.66, \bar{\lambda}_2 = 0.68, \bar{\lambda}_3 = 0.5, \kappa_1 = 0.8, \kappa_2 = 0.6, \kappa_3 = 0.4, \eta_1 = 0.8, \eta_2 = 0.13, \eta_3 = 0.12, \mu_1 = 0.22, \mu_2 = 0.25, \mu_3 = 0.11, \xi_1 = 0.33, \xi_2 = \xi_3 = 0.22, a_1 = 24, a_2 = a_3 = 17.6, \tau_1 = 0.06, \tau_2 = 0.02, \tau_3 = 0.04$, and the parameters of radial basis function neural networks are the same as ones in Example 1. The initial values are chosen as $x(0) = (-0.1, 0.4, -0.6)$ and $\hat{\theta}_1(0) = 2.2, \hat{\theta}_2(0) = \hat{\theta}_3(0) = 5.6$.

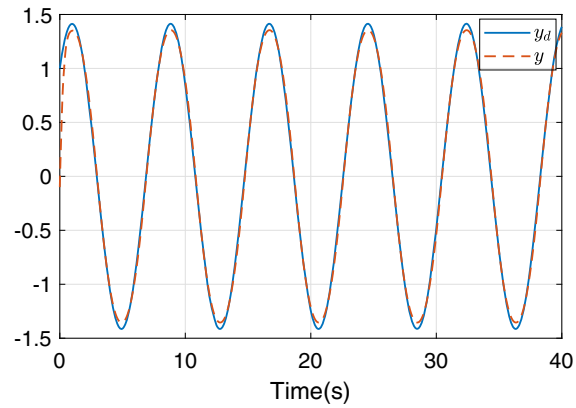

Fig. 8 Trajectories of reference signal y_d and output y

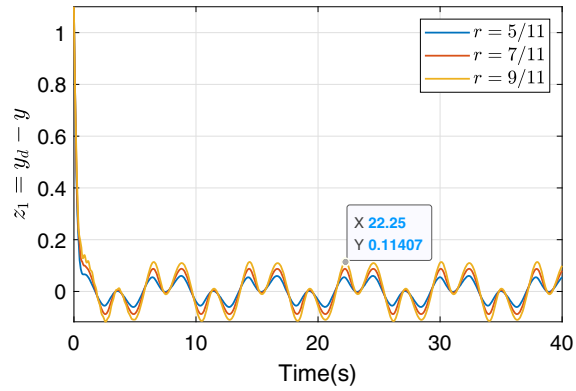

Fig. 9 Trajectory of tracking error $z_1 = y_d - y$

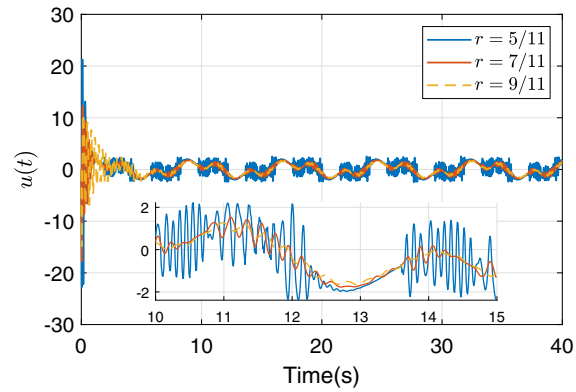

Fig. 10 Trajectories of system input u

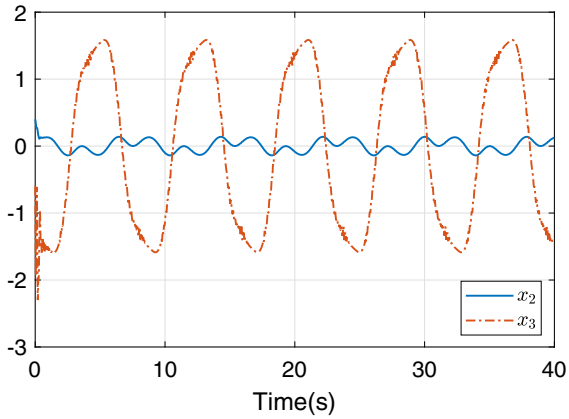

Fig. 11 Trajectories of state variables x_2 and x_3

The simulation results are presented in Figs. 8, 9, 10, 11, 12 and 13. Figures 8 and 9 give the system output y and the corresponding tracking error z_1 ($r = \frac{5}{11}$), from which we see that the proposed practical finite-time control scheme can effectively control system (38) to achieve the tracking objective. As pointed out in Remark 8, r is an important parameter in the proposed practical finite-time control scheme. Thus, we choose the different r ($r = \frac{7}{11}$ and $\frac{9}{11}$) and compare the tracking error z_1 and the system input u. From Figs. 9 and 10, we see that a small r implies a small tracking error, while the fluctuation range of the control input u becomes large with the reduction of r, i.e., the large control force is needed. Thus, in practice, it is necessary to make a trade-off between the tracking performance and control force according to the actual engineering requirements. The state variables x_2, x_3 and the estimated parameters $\hat{\theta}_1, \hat{\theta}_2, \hat{\theta}_3$ are presented in Figs. 11 and 12, respectively. Figure 13 gives the virtual control signals χ_1, χ_2 and the compensated signals $\tilde{\chi}_1$, $\tilde{\chi}_2$, $\tilde{\chi}_3$. Based on Figs. 8, 9, 10, 11, 12 and 13, we also know that all signals in the closed-loop system (38) are bounded, which indicates the effectiveness of the proposed control scheme.

Remark 11 In some existing literature, such as [18,36,37], the input signal u has a large fluctuation around the initial time, which may be unreasonable and unacceptable in practice. Unlike the aforementioned literature, the control input u in this paper is generated by a filter and thus the fluctuation range of u can be reduced, which is also illustrated by two numerical examples. More precisely, the signal h_3 in this paper has a similar form with the control input in [18,36,37], so we compare the difference between h_3 and u, and the results are shown in Fig. 14 for Examples 1 and 2. From Fig. 14, we see that the fluctuation range of u is significantly lower than that of h_3 for both practical finite-time and non-finite time control schemes, especially around the initial time. Therefore, the proposed control scheme has an apparent effect on reducing the fluctuation range of the input signal. In addition, the difference between h_3 and u is large, and should not be neglected, which indicates that the introduction of compensated signal $\tilde{\chi}_i$ is needed and reasonable.

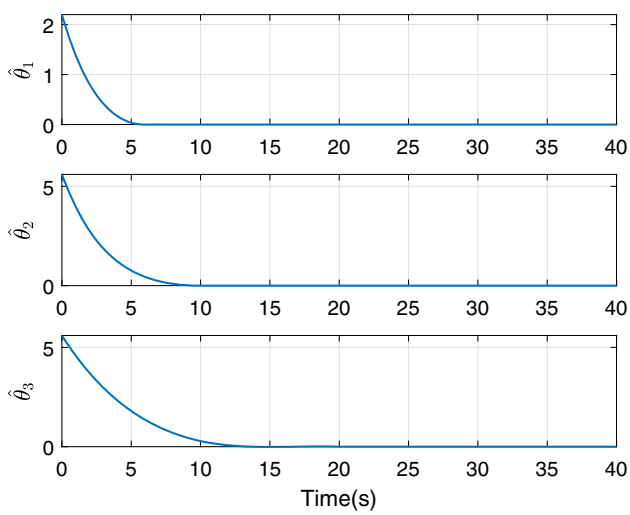

Fig. 12 Trajectories of estimated parameter $\hat{\theta}_i$

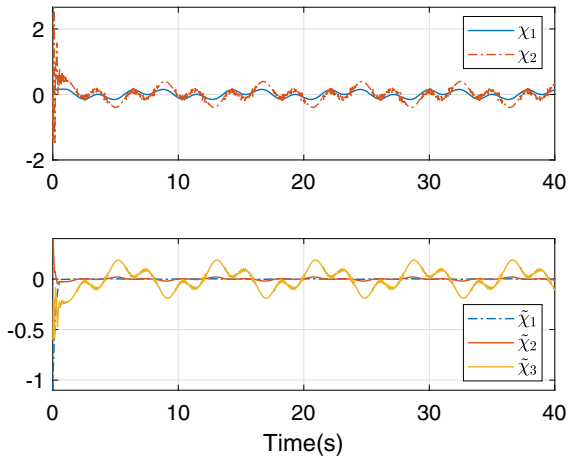

Fig. 13 Trajectories of virtual control signals χ_1, χ_2 and compensated signals $\tilde{\chi}_i$

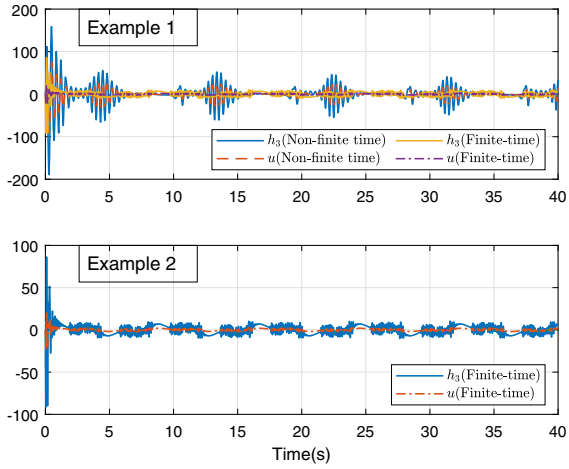

Fig. 14 Trajectories of system input u and intermediate signal h_3 in Examples 1 and 2

5 Conclusion

In this paper, the issue associated with the practical finite-time adaptive neural networks control has been considered for a class of incommensurate FOS with external disturbances. With the help of the established practical finite-time stability criterion and the property of fractional-order calculus, a practical finite-time adaptive control scheme has been designed for an incommensurate FOS, where the control signals are generated by some designed filters. During the design processes of the control scheme, a compensated signal has been introduced to compensate for the difference from the filters of control signals, and thus, the design processes of the control scheme and stability analysis have been simplified. The proposed control scheme provides a new way for the practical finite-time adaptive control of FOSs, while the constraint on the derivative-order α_i (i.e., Assumption 3) brings some limitations on the practical applications of the proposed control scheme, which inspires us to study how to remove this assumption in the future. In addition, to highlight the novelty of the proposed practical finite-time control scheme, only a classical incommensurate fractional-order nonlinear system has been considered in this paper. Thus, we expect to extend the practical finite-time control scheme to a more general and practical system in the future.

Acknowledgements This work was jointly supported by the National Natural Science Foundation of China under Grant Nos. 61673111 and 61833005, and the National Key Research and Development Program of China under Grant No. 2018AAA0100202.

Funding National Natural Science Foundation of China (Grant Nos. 61673111 and 61833005), National Key Research and Development Program of China (Grant No. 2018AAA0100202).

Data availability Data sharing is not applicable to this article as no datasets were generated or analyzed during the current study.

Compliance with ethical standards

Conflict of interest The authors declare that they have no conflict of interest.

References

1. Podlubny, I.: Fractional Differential Equations. Academic Press, San Diego (1999)
2. Petráš, I.: Fractional-Order Nonlinear Systems: Modeling, Analysis and Simulation. Springer, Berlin (2011)
3. Wu, F., Li, F., Chen, P., Wang, B.: Finite-time control for a fractional-order non-linear HTGS. IET Renew. Power Gen. **13**(4), 633–639 (2019)
4. Yao, X., Liu, Y., Zhang, Z., Wan, W.: Synchronization rather than finite-time synchronization results of fractional-order multi-weighted complex networks. IEEE Trans. Neural Netw. Learn. Syst. (2021). https://doi.org/10.1109/tnnls.2021.3083886
5. Liu, S., Zhao, S., Niu, B., Li, J., Li, H.: Stability analysis of a nonlinear electromechanical coupling transmission system with time delay feedback. Nonlinear Dyn. **86**(3), 1863–1874 (2016)
6. Yang, D., Zong, G., Su, S.-F., Liu, T.: Time-driven adaptive control of switched systems with application to electro-hydraulic unit. IEEE Trans. Cybern. **52**(11), 11906–11915 (2021)

7. Cao, B., Nie, X., Wu, Z., Xue, C., Cao, J.: Adaptive neural network control for nonstrict-feedback uncertain nonlinear systems with input delay and asymmetric time-varying state constraints. J. Frankl. Inst. **358**(14), 7073–7095 (2021)
8. Yang, W., Yu, W., Lv, Y., Zhu, L., Hayat, T.: Adaptive fuzzy tracking control design for a class of uncertain nonstrict-feedback fractional-order nonlinear SISO systems. IEEE Trans. Cybern. **51**(6), 3039–3053 (2021)
9. Song, S., Park, J.H., Zhang, B., Song, X.: Observer-based adaptive hybrid fuzzy resilient control for fractional-order nonlinear systems with time-varying delays and actuator failures. IEEE Trans. Fuzzy Syst. **29**(3), 471–485 (2021)
10. Wang, X., Jiang, K., Zhang, G., Niu, B.: Event-triggered-based adaptive decentralized asymptotic tracking control scheme for a class of nonlinear pure-feedback interconnected systems. Nonlinear Dyn. **104**, 3881–3895 (2021)
11. Zhang, T., Ge, S.S.: Adaptive neural network tracking control of MIMO nonlinear systems with unknown dead zones and control directions. IEEE Trans. Neural Netw. **20**(3), 483–497 (2009)
12. Li, D., Li, D.: Adaptive tracking control for nonlinear time-varying delay systems with full state constraints and unknown control coefficients. Automatica **93**, 444–453 (2018)
13. Chen, B., Zhang, H., Lin, C.: Observer-based adaptive neural network control for nonlinear systems in nonstrict-feedback form. IEEE Trans. Neural Netw. Learn. Syst. **27**(1), 89–98 (2016)
14. Cao, B., Nie, X.: Observer-based adaptive neural networks control for Markovian jump nonlinear systems with partial mode information and input saturation. Int. J. Robust Nonlinear Control **31**(14), 6880–6904 (2021)
15. Zhang, T., Lin, M., Xia, X., Yi, Y.: Adaptive cooperative dynamic surface control of non-strict feedback multi-agent systems with input dead-zones and actuator failures. Neurocomputing **442**, 48–63 (2021)
16. Zhang, J., Niu, B., Wang, D., Wang, H., Duan, P., Zong, G.: Adaptive neural control of nonlinear nonstrict feedback systems with full-state constraints: a novel nonlinear mapping method. IEEE Trans. Neural Netw. Learn. Syst. (2021). https://doi.org/10.1109/tnnls.2021.3104877
17. Li, Y., Tong, S.: Adaptive fuzzy output constrained control design for multi-input multioutput stochastic nonstrict-feedback nonlinear systems. IEEE Trans. Cybern. **47**(12), 4086–4095 (2017)
18. Li, Y.-X., Wang, Q.-Y., Tong, S.: Fuzzy adaptive fault-tolerant control of fractional-order nonlinear systems. IEEE Trans. Syst. Man Cybern. Syst. **51**(3), 1372–1379 (2021)
19. Li, X., Wen, C., Zou, Y.: Adaptive backstepping control for fractional-order nonlinear systems with external disturbance and uncertain parameters using smooth control. IEEE Trans. Syst. Man Cybern. Syst. **51**(12), 7860–7869 (2021)
20. Liu, H., Pan, Y., Cao, J.: Composite learning adaptive dynamic surface control of fractional-order nonlinear systems. IEEE Trans. Cybern. **50**(6), 2557–2567 (2020)
21. Ma, Z., Ma, H.: Adaptive fuzzy backstepping dynamic surface control of strict-feedback fractional-order uncertain nonlinear systems. IEEE Trans. Fuzzy Syst. **28**(1), 122–133 (2020)
22. Cao, B., Nie, X.: Event-triggered adaptive neural networks control for fractional-order nonstrict-feedback nonlinear systems with unmodeled dynamics and input saturation. Neural Netw. **142**, 288–302 (2021)
23. Gong, P., Han, Q.-L., Lan, W.: Finite-time consensus tracking for incommensurate fractional-order nonlinear multi-agent systems with directed switching topologies. IEEE Trans. Cybern. **52**(1), 65–76 (2022)
24. Gong, P., Han, Q.-L.: Practical fixed-time bipartite consensus of nonlinear incommensurate fractional-order multiagent systems in directed signed networks. SIAM J. Control. Optim. **58**(6), 3322–3341 (2020)
25. Wang, C., Liang, M., Gao, J.: Adaptive fuzzy output tracking control of a class of uncertain fractional order systems subject to unknown disturbance. IEEE Access **6**, 70655–70665 (2018)
26. Wang, C., Liang, M., Chai, Y.: Adaptive control of a class of incommensurate fractional order nonlinear systems with input dead-zone. IEEE Access **7**, 153710–153723 (2019)
27. Wang, C., Liu, X., Wang, H.: An adaptive fault-tolerant control scheme for a class of fractional-order systems with unknown input dead-zones. Int. J. Syst. Sci. **52**(2), 291–306 (2020)
28. Bhat, S.P., Bernstein, D.S.: Finite-time stability of continuous autonomous systems. SIAM J. Control. Optim. **38**(3), 751–766 (2000)
29. Yu, S., Yu, X., Shirinzadeh, B., Man, Z.: Continuous finite-time control for robotic manipulators with terminal sliding mode. Automatica **41**(11), 1957–1964 (2005)
30. Zhu, Z., Xia, Y., Fu, M.: Attitude stabilization of rigid spacecraft with finite-time convergence. Int. J. Robust Nonlinear Control **21**(6), 686–702 (2011)
31. Yu, J., Shi, P., Zhao, L.: Finite-time command filtered backstepping control for a class of nonlinear systems. Automatica **92**, 173–180 (2018)
32. Cui, B., Xia, Y., Liu, K., Shen, G.: Finite-time tracking control for a class of uncertain strict-feedback nonlinear systems with state constraints: a smooth control approach. IEEE Trans. Neural Netw. Learn. Syst. **31**(11), 4920–4932 (2020)
33. Shang, Y., Chen, B., Lin, C.: Fast finite-time adaptive neural control of multi-agent systems. J. Frankl. Inst. **357**(15), 10432–10452 (2020)
34. Song, S., Zhang, B., Xia, J., Zhang, Z.: Adaptive backstepping hybrid fuzzy sliding mode control for uncertain fractional-order nonlinear systems based on finite-time scheme. IEEE Trans. Syst. Man Cybern. Syst. **50**(4), 1559–1569 (2020)
35. Yang, S., Yu, J., Hu, C., Jiang, H.: Finite-time synchronization of memristive neural networks with fractional-order. IEEE Trans. Syst. Man Cybern. Syst. **51**(6), 3739–3750 (2021)
36. Li, Y.-X., Wei, M., Tong, S.: Event-triggered adaptive neural control for fractional-order nonlinear systems based on finite-time scheme. IEEE Trans. Cybern. **52**(9), 9481–9489 (2022)
37. Wei, M., Li, Y.-X., Tong, S.: Adaptive fault-tolerant control for a class of fractional order non-strict feedback nonlinear systems. Int. J. Syst. Sci. **52**(5), 1014–1025 (2020)
38. Diethelm, K.: The Analysis of Fractional Differential Equations. Springer, Berlin (2010)
39. Xi, Q., Liu, X.: Finite-time stability and controller design for a class of hybrid dynamical systems with deviating argument. Nonlinear Anal. Hybrid Syst. **39**, 100952 (2021)

40. Zhang, J., Li, S., Ahn, C.K., Xiang, Z.: Sampled-data output voltage regulation for a DC–DC buck converter nonlinear system with actuator and sensor failures. Nonlinear Dyn. **99**(2), 1243–1252 (2019)
41. Girosi, F., Poggio, T.: Networks and the best approximation property. Biol. Cybern. **63**(3), 169–176 (1990)
42. Gong, P., Lan, W., Han, Q.-L.: Robust adaptive fault-tolerant consensus control for uncertain nonlinear fractional-order multi-agent systems with directed topologies. Automatica **117**, 109011 (2020)